Kinetic Modeling of CO2 Biofixation by Microalgae and Optimization of Carbon Supply in Various Photobioreactor Technologies

Jeremy Pruvost, Benjamin Le Gouic, Jean-François Cornet

ACS Sustainable Chemistry & Engineering

pubs.acs.org/journal/ascecg

Research Article

Kinetic Modeling of CO_2 Biofixation by Microalgae and Optimization of Carbon Supply in Various Photobioreactor Technologies

Jeremy Pruvost,* Benjamin Le Gouic, and Jean-François Cornet

Cite This: *ACS Sustainable Chem. Eng.* 2022, 10, 12826−12842

Read Online

ACCESS | Metrics & More | Article Recommendations

ABSTRACT: Photosynthetic microorganisms like microalgae or cyanobacteria can be used to fix CO_2 from industrial effluents in a sustainable way. However, the gaseous CO_2 must be first transferred into the liquid phase in the form of dissolved inorganic carbon (DIC) to then be assimilated and thus biofixed by microalgae. This article introduces and validates a model able to relate effects of those parameters on relevant quantities, such as CO_2 biofixation rates and CO_2 use efficiency as characterized by CO_2 removal from the gas phase. The ability to predict carbon fluxes in the process as a function of operating parameters is first illustrated for lab-scale photobioreactors, emphasizing the difficulty to optimize both CO_2 biofixation rates (which implies maximizing biomass growth) and CO_2 removal from the gas phase (which implies working at low DIC concentrations). As two technologies presenting different gas−liquid mass transfer performances, mechanically stirred versus airlift systems are then discussed. Covered raceways are revealed to be of interest, reaching up to 80% in CO_2 use efficiency, while the large flow rate needed for sufficient mixing in airlift systems facilitates the CO_2 supply to the culture to the detriment of CO_2 use efficiency, typically only a few percent in usual operating conditions. Finally, the potential of a multistage strategy is investigated for a typical CO_2-enriched flue gas. The relevance of biological fixation as a carbon sink and of system arrangement (i.e., series, parallel, or in combination) will be discussed in terms of biomass production, surface requirement, and carbon removal efficiency.

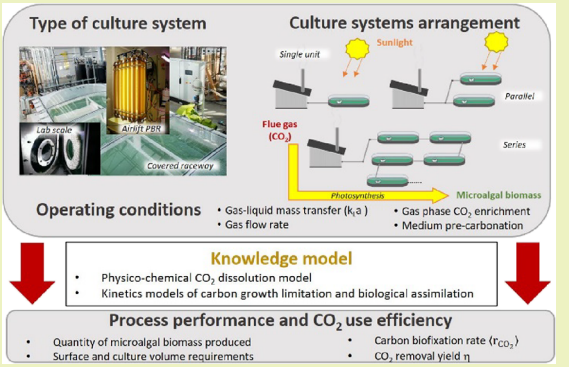

KEYWORDS: *microalgae, CO_2, biofixation, photobioreactors, modeling, flue gas*

INTRODUCTION

Photosynthetic microorganisms like microalgae and cyanobacteria fix CO_2 when grown in autotrophic culture condition. They appear then as a solution of interest to convert CO_2 from different sources including the atmosphere and industrial exhaust gases into valuable products, contributing to reduce greenhouse gas emissions into the atmosphere.[1−4]

Gaseous CO_2 is not directly assimilated by photosynthetic microorganisms and need to be first transferred to the culture medium to form dissolved inorganic carbon (DIC) that is then assimilated by photosynthetic microorganisms. A sufficient inorganic carbon supply is also needed to avoid growth limitation by the carbon source and then maintain maximal assimilation through the photosynthesis process. As a result, both DIC concentration and the kinetics of CO_2 dissolution are relevant in the culture process:[5] (i) low DIC concentration values reduce growth rate and induce carbon concentration mechanisms in the cell, and (ii) the kinetics of CO_2 dissolution has to be large enough to maintain a sufficient DIC concentration to avoid growth limitation. DIC concentration is determined by carbon chemistry and mainly depends on the pH value of the liquid phase and parameters affecting gas−liquid mass transfer, such as gas flow rate and molar fraction of gaseous CO_2 in the inlet.

In practice, it is rather simple to maintain a sufficient DIC concentration to avoid growth limitation in culture systems by enriching the culture medium with carbonates or the gas phase in CO_2 (a few percent is sufficient) and controlling DIC concentration through pH regulation.[6] However, maximal growth does not guarantee an optimal use of the CO_2. Such optimization is however relevant (i) to decrease, for example, the operating cost of a commercial application (the cost related to carbon supply being afford for around 20−40% of the operating cost in some cases; see ref 7) or (ii) to decrease CO_2 re-emitted in the outlet gaseous phase in the perspective of using photosynthetic microorganisms as a way to valorize flue gas through microalgal biomass various applications.[3,4,8] The

Received: July 1, 2022
Revised: August 29, 2022
Published: September 15, 2022

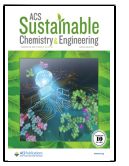

carbon fate in the process, such as the carbon absorption/desorption phenomena that occur in culture systems, is of interest here.[5]

In a previous work, the authors have presented an experimental setup for the detailed investigation of the effects of carbon limitation of the photosynthetic microalgae growth.[5] This allowed measuring various carbon fluxes involved during cultivation of the microalga *Chlorella vulgaris*. Those carbon fluxes were then modeled, enabling obtaining a detailed representation of complex interactions between biological (growth and then carbon biological consumption) and physical (gas−liquid mass transfer) kinetics, both affecting the DIC concentration and then the resulting growth. For insufficient gas enrichment, effects of carbon limitation by DIC concentration were clearly established, with a decrease in biomass concentration and productivity and, as a result, CO_2 biofixation rate for DIC concentrations lower than 0.5−1 mM. In contrast, for nonlimiting value of the carbon supply, a maximal growth rate (and then carbon biofixation rate) as limited by the light supply was observed, leading to DIC accumulation in the culture medium and progressive decrease of the gaseous CO_2 mass transfer to the liquid phase, resulting in poor efficiency in CO_2 use.

The following work will extend our knowledge model of the physicochemical CO_2 dissolution model that was validated in our previous work by introducing the biological carbon consumption and growth kinetics limitation by DIC concentration. This will enable one to predict relevant features for optimal CO_2 use in microalgae-based bioprocesses, like carbon biofixation rates and CO_2 abatement in the gas phase. The model will be validated onto experimental data and then used to investigate various strategies to optimize carbon use and fixation through photosynthetic microorganisms' culture. To emphasize the role of mixing in CO_2 supply to the culture volume (i.e., gas−liquid mass transfer), different cultivation systems such as mechanically stirred (i.e., lab-scale torus-shaped PBR and covered raceway for solar culture) and airlift culture systems will be simulated. Finally, the potential of a multistage strategy CO_2-enriched flue gas will be demonstrated.

EXPERIMENTAL SECTION

Experimental results given in Le Gouic et al.[5] were used to adjust the growth kinetic model. Only main experimental features are given here.

Culture data were obtained in a fully controlled lab-scale torus-shaped PBR, which (i) allows a rigorous control of all growing conditions (light, temperature, medium composition), (ii) is mechanically stirred to provide an accurate analysis of the gas phase in the PBR outlet, (iii) is equipped with a pH acid/base regulation to disconnect CO_2 dissolution from pH evolution, and (iv) is equipped with a CO_2 analyzer (SIEMENS Ultramat 6E) and a complete set of gas mass flowmeters. The potential of this experimental setup to obtain online an accurate carbon mass balance during microalgae culture was validated with *Chlorella vulgaris* (211/19 CCAP), which was also retained as a case study in this work.

Data used to adjust the model were obtained in continuous mode, with constant pH and temperature controlled at 7.5 and 25 °C, respectively. *Chlorella vulgaris* was cultivated in an autotrophic medium based on the Sueoka medium.[5]

THEORY/CALCULATION

Modeling of Carbon Mass Transfer and of Carbon Growth Limitation. *Introduction.* The physicochemical modeling of the CO_2 gas−liquid mass transfer in a microalgal culture system was already presented in Le Gouic et al.[5] It was especially shown that attention should be paid on the carbon dissolution chemistry and its relation to pH value. This model was validated against various absorption/desorption experiments. As an important asset of the combination of the model with the monitoring applied on our experimental setup, the gas−liquid mass transfer coefficient (k_La) was measured online. In this work, we propose to extend this model by introducing the relation to microalgae growth kinetics to predict culture systems' performances for various carbon feeding strategies. At this stage, it is important to note that all the reasoning and analyses that follow in this article are based on two fundamental assumptions:

(i) It has been well known since the 1980s that the dissolved carbon source of microalgae and cyanobacteria is bicarbonate (Coleman and Colman, 1981). This fact has been studied and confirmed since this period (Salbitani et al., 2020), including to establish air CO_2 mitigation strategies (Zhu et al., 2020);

(ii) Within the liquid phase of a photobioreactor, dissolved species such as CO_2 or bicarbonate ions are considered at each time at the thermodynamic equilibrium (quasi steady-state hypothesis, see Le Gouic et al., 2021).[5] It is therefore equivalent to reason with dissolved CO_2, bicarbonate or even with total dissolved inorganic carbon (C_T or DIC in this article) if working in moles (as explained in the following part).

Modeling of CO_2 Gas−Liquid Mass Transfer into the Culture System. Because of the carbon dissociation in liquids, it is useful to introduce C_T, the total concentration in dissolved inorganic carbon (DIC), as a reference:

$$C_T = \mathrm{DIC} = C_{CO_2,L} + C_{HCO_3^-} + C_{CO_3^{2-}} = K\, C_{CO_2,L} \quad (1)$$

where C_T is directly related to CO_2 dissolved concentration by the dissolution equilibrium constant K, which is mainly related to pH and temperature values (see Le Gouic et al.[5]).

The biological consumption rate can be introduced in a carbon mass balance, which enables one to also relate C_T to gas−liquid mass transfer, input (feed), and output (harvest) from the liquid phase:

$$\frac{dC_T}{dt} = k_La\left(C^*_{CO_2,L} - \frac{\mathbf{C_T}}{\boldsymbol{K}}\right) - \langle r_{CO_2}\rangle + \frac{(C^i_T - C_T)}{\tau_p} \quad (2)$$

where $\langle \boldsymbol{r}_{CO_2}\rangle$ is the carbon biological consumption rate by photosynthetic growth (here expressed in mole, with $\langle \boldsymbol{r}_{CO_2}\rangle = \langle \boldsymbol{r}_x\rangle$ if $\langle \boldsymbol{r}_x\rangle$ is expressed in C-mol; see eq 5), $\boldsymbol{C}^*_{CO_2,L}$ the dissolved carbon concentration at thermodynamic equilibrium with the gas phase, τ_p the residence time resulting from the liquid flow rate of the feed (fresh medium) (with $\tau_p = 1/D$, where D is the dilution rate), and $\mathbf{C}^i_T$ the total DIC concentration in the feeding medium.

A perfectly mixed mass balance on the gas phase at quasi steady-state leads to the following equation:

$$N_{CO_2} = \frac{\boldsymbol{G}}{\boldsymbol{V_L}}\cdot(\boldsymbol{y}^i_{CO_2} - \boldsymbol{y}^o_{CO_2}) = \frac{G}{V_L}\cdot\Delta y_{CO_2}$$
$$= k_La\left(\mathbf{C}^*_{CO_2,L} - \frac{\mathbf{C_T}}{\boldsymbol{K}}\right) = k_La\cdot\left(\frac{y^o_{CO_2}\cdot P}{H} - \frac{C_T}{K}\right) \quad (3)$$

where N_{CO_2} is the volumetric molar flux between gas and liquid phases, H is Henry's constant, P is the total pressure, G is the gas flow rate, V_L is the culture volume, and $\boldsymbol{y}^i_{CO_2}$ and $\boldsymbol{y}^o_{CO_2}$ are the CO_2

https://doi.org/10.1021/acssuschemeng.2c03927
ACS Sustainable Chem. Eng. 2022, 10, 12826−12842

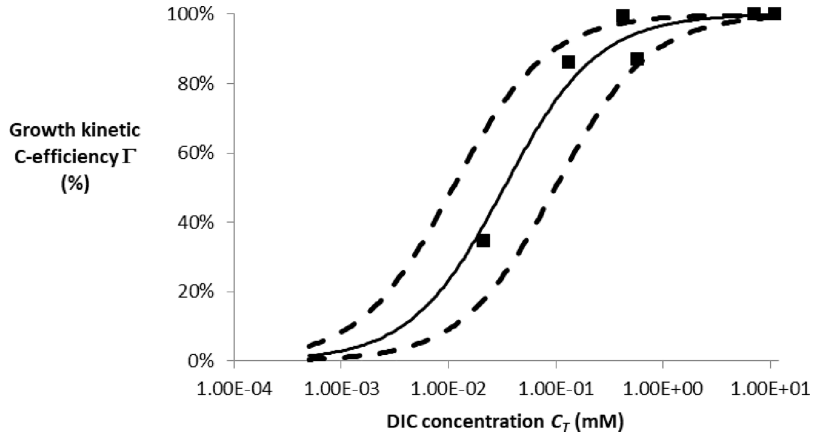

Figure 1. Modeling of the kinetic growth limitation of *Chlorella vulgaris* by the carbon source (PFD = 250 μmol·m^{-2}·s^{-1}, T = 25 °C, pH = 7.5). Experimental data (black squares) are obtained from continuous culture in torus-shaped PBR (Le Gouic et al. 2021),[5] and a Monod-like relation is used for modeling with K_{DIC} = 0.033 mM (full line). Dashed lines correspond to values of the saturation constant K_{DIC} used in the sensitivity analysis ($3K_{DIC}$ and $K_{DIC}/3$ for the lower and upper curve, respectively; see text for details).

content in the inlet and outlet of the culture system, respectively. Note that carbon accumulation in the gas phase was neglected here because a sufficient constant flow rate was supposed together with a lower time constant for the gas phase balance in comparison to the liquid phase balance, as usually obtained in practice (see Le Gouic et al.[5] for more details).

Equation 3 indicates that the variation in CO_2 molar flow rate between the culture system inlet and outlet is due to the CO_2 mass transfer from the gas to the liquid phase (which is then possibly consumed by microalgae, as represented by $\langle r_{CO_2}\rangle$ in eq 2). Please note that eq 3 also demonstrates that the gas−liquid mass transfer coefficient k_La can be directly retrieved with high accuracy from carbon concentration measurements on both liquid and gas phases. Such property was demonstrated in our previous work.[5]

By combining eqs 2 and 3, we obtain in steady state (i.e., constant C_T value)

$$\langle r_{CO_2}\rangle = k_La\left(C^*_{CO_2,L} - \frac{C_T}{K}\right) + \frac{(C^i_T - C_T)}{\tau_p} = \frac{G}{V_L}(y^i_{CO_2} - y^o_{CO_2}) + \frac{(C^i_T - C_T)}{\tau_p} \quad (4)$$

The biological carbon consumption rate $\langle r_{CO_2}\rangle$ is related to the biomass volumetric growth rate. For a perfectly mixed culture system operated in continuous mode and at steady state, the volumetric growth rate is equal to the biomass volumetric productivity P_x:

$$\langle r'_x\rangle = P_x = C_x/\tau_p = C_x D, \quad (5)$$

with $<r'_x>$ is the mean volumetric biomass production rate in the culture system (here expressed in mass). C_x represents here the concentration of biomass totally produced, which is the sum of the dry-weight concentration (as usually obtained after filtering, drying, and weighting a culture volume) and the exudates obtained in dissolved form (i.e., dissolved organic carbon). For *Chlorella vulgaris* and under the culture conditions investigated, exudate production was found to be proportional to the dry-weight concentration (around 8% of the dry-weight concentration, data not shown).

The volumetric productivity of the biomass (i.e., biomass growth rate, including dry-weight and dissolved organic carbon concentrations) is also related to the mass yield of biological consumption of CO_2 (in kg CO_2/kg dry mass):

$$Y_{CO_2/X} = \frac{\langle r_{CO_2}\rangle M_{CO_2}}{\langle r'_X\rangle} \quad (6)$$

with M_{CO_2} the molar mass of CO_2.

Combining eqs 6 and 4 at steady state leads to

$$\langle r_{CO_2}\rangle = \frac{Y_{CO_2/X}}{M_{CO_2}}\langle r'_X\rangle = \frac{Y_{CO_2/X}}{M_{CO_2}}P_x = k_La\left(C^*_{CO_2} - \frac{C_T}{K}\right) + \frac{(C^i_T - C_T)}{\tau_p} = \frac{G}{V_L}.(y^i_{CO_2} - y^o_{CO_2}) + \frac{(C^i_T - C_T)}{\tau_p} \quad (7)$$

This equation indicates that if carbon concentrations are monitored, the biological growth rate $\langle r'_X\rangle$ can be determined online from gas and liquid phase monitoring (or at least the biological consumption rate $\langle r_{CO_2}\rangle$ if the conversion yield $Y_{CO_2/X}$ is not assumed to be constant). Retrospectively, once the gas−liquid mass transfer coefficient and biological growth rate are known (from measurement or model prediction as described in the next section), all carbon concentrations (C_T and $y^o_{CO_2}$) can be determined for given operating parameters (gas flow rate G, injected carbon concentrations in both liquid and gas feeds). All carbon fluxes can then be deduced for a complete characterization of the process, enabling one to determine various quantities such as (i) the volumetric flow of CO_2 transferred to the liquid phase N_{CO_2}(i.e., $\frac{G}{V_L}(y^i_{CO_2} - y^o_{CO_2})$, eq 3; hereafter named the CO_2 transfer rate N_{CO_2}), (ii) the biological CO_2 consumption rate $\langle r_{CO_2}\rangle$ (i.e., $\langle r_{CO_2}\rangle = \frac{G}{V_L}.(y^i_{CO_2} - y^o_{CO_2}) + \frac{(C^i_T - C_T)}{\tau_p}$, eq 7; hereafter named the CO_2 biofixation rate), and (iii) the CO_2 removal yield η to quantify the percentage of gaseous CO_2 transferred in the culture system for either biomass synthesis or accumulation in liquid phase:[9]

https://doi.org/10.1021/acssuschemeng.2c03927
ACS Sustainable Chem. Eng. 2022, 10, 12826−12842

$$\eta = \frac{y^{i}_{CO_2} - y^{o}_{CO_2}}{y^{i}_{CO_2}} = \frac{\Delta y_{CO_2}}{y^{i}_{CO_2}} \quad (8)$$

Modeling of the Photosynthetic Growth Rate. Prediction of biomass (eq 5) and dissolved carbon concentrations (eq 2) for given operating conditions requires knowledge of the biomass volumetric growth rate ($\langle r'_X \rangle$) (eq 7). This is not straightforward as light attenuation in microalgae culture systems implies consideration of the relation between light availability in the culture volume and the photosynthetic growth.[10−15] As a fundamental aspect of PBR modeling, this was extensively described by authors, and the same methodology will be applied here by using the model described by Soulies et al.[16] for *Chlorella vulgaris* in light-limited growth (i.e., all nutrients including carbon were provided in excess). This approach based on knowledge models for both photosynthetic growth and radiative transfer was indeed proven to be able to predict biomass growth in several PBR configurations such as the torus-shaped PBR used in this study for various illumination conditions including white and red light spectra and normal and oblique incident angles while taking into account some relevant biological features like pigment acclimation.[16] It was then used in this study with no further adjustment except for carbon limitation, which was introduced here (see Section Modeling of Carbon Limitation Effects).

The overall model was solved by using the Matlab software (ode15s). Once the growth rate was predicted, CO_2 content in the gas outlet $y^{o}_{CO_2}$ and DIC concentration C_T in the culture medium were determined as a function of operating parameters. In all cases, an initial guess of those values was given for better model convergence. DIC was fixed to a null value, and $y^{o}_{CO_2}$, which was found to be sensitive in the convergence process, was estimated from the mass balance between gas and liquid phases (eq 3), which allows providing an initial guess of the value respecting the overall carbon mass balance.

RESULTS AND DISCUSSION

Modeling of Carbon Limitation Effects. Figure 1 was obtained from the data given in Le Gouic et al.[5] Biomass productivities were obtained in a lab-scale torus-shaped PBR for various DIC concentrations, as obtained by varying the CO_2 gas composition so as to increase carbon transferred from the gas to the liquid phase and then DIC concentration. Those data were obtained at a constant photon flux density (i.e., PFD) of 250 μmol·m^{-2}·s^{-1} for the steady state in a continuous culture. Special attention was paid to obtain a constant DIC concentration for a representative measurement of the DIC concentration influence on the growth rate. To emphasize carbon growth limitation by DIC concentration, results here are expressed as the growth kinetic C-efficiency Γ (given in %), which represents the ratio of the biomass productivities achieved in carbon limiting conditions ($<r'^{CL}_X>$) over conditions only limited by light ($<r'^{LL}_X>$ corresponding to the maximum growth rate for the given incident PFD.[5]

Results tend to emphasize a growth limitation by the carbon source for DIC values lower than 0.5−1 mM at pH 7.5, with then a sudden decrease of the resulting growth rate. As already discussed in Le Gouic et al.[5] through a detailed analysis, there was no relevant variation in cells' biochemical composition except for the pigment content that could be accounted for by the variation in light attenuation conditions as a consequence of biomass concentration and growth kinetics decrease. Consequently, an almost constant value of $Y_{CO_{2/X}}$ around 1.8 ± 0.07 was obtained even in carbon limited conditions, close then to the theoretical value of 1.76 obtained from the biomass elementary analysis.[5,17]

Based on the evolution of the growth rate with DIC concentration C_T presented in Figure 1, the carbon limitation was represented in the first instance by a Monod growth model, which is usually applied to represent nutrient-limited growth:[18]

$$<r'_X> = <r'^{LL}_X> \cdot \frac{C_T}{C_T + K_{DIC}} \quad (9)$$

where $<r'^{LL}_X>$ is the growth rate (i.e., biomass productivity) obtained for the condition where light only limits growth. $<r'^{LL}_X>$ was then calculated from the predictive model presented in Soulies et al.[16] by considering operating conditions and PBR geometrical characteristics used in Le Gouic et al.,[5] leading to $<r'^{LL}_X> = 1.6 \times 10^{-2}$ g·L^{-1}·h^{-1} (i.e., PFD of 250 μmol·m^{-2}·s^{-1}, PBR depth of 0.04 m, corresponding to an areal biomass productivity $S_X = 15.4$ g·m^{-2}·day^{-1}).

The growth modeling was added in Figure 1 by using a saturation constant K_{DIC}= 0.033 mM that was obtained by error minimization. Although a rather good agreement is observed, some important comments have to be mentioned:

- As for any Monod-like relation, this relation is only valid in the conditions of our investigation (PFD = 250 μmol$_{h\nu}$·m^{-2}·s^{-1}, T = 25 °C, pH = 7.5). Any change such as in PFD could indeed lead to a different biological demand in carbon to sustain growth activity, which may influence the growth−CID relation observed in this study. This is clearly a weakness when considering the large applicability of the kinetic model used for predicting light-limited growth.
- The model can be considered as oversimplified regarding complex mechanisms involved in the condition of carbon limitation, like the numerous carbon concentration mechanisms involved in microalgae.[19] However, at the process level, we observed that carbon limitation mainly resulted in a decrease in growth kinetics.
- It can be argued that there were an insufficient number of data for DIC concentration where growth limitation occurs (<1 mM), leading to a possible inaccuracy in the determination of the saturation constant K_{DIC} and then in model predictions. A sensitivity analysis on prediction results toward the K_{DIC} value was then conducted. Figure 1 gives a Monod-like relation for the two other values of K_{DIC} used in this analysis (i.e., $K_{DIC}/3$ and $3K_{DIC}$), which were found to be good upper and lower bounds for the prediction of experimental values. As will be demonstrated, a rather moderate influence was found in the key-predicted values of the process, as explained by our general aim to find enrichment strategies to optimize growth and then CO_2 biofixation rate, with DIC concentration C_T then usually higher than 1 mM (where the Monod-type relation $\frac{C_T}{C_T + K_{DIC}}$ is close to 1). Further refinement in the estimation of K_{DIC} value was then considered unnecessary.

Despite its limitations, our simple modeling with a Monod-type formulation was then considered acceptable in the first instance. Future studies should however aim to improve this aspect by aiming to develop a knowledge model able to

https://doi.org/10.1021/acssuschemeng.2c03927
ACS Sustainable Chem. Eng. 2022, 10, 12826−12842

Table 1. Validation of the Model[a]

experimental data	#1	#2	#3	#4
residence time (h)	27.25	27.7	69.44	72.5
CO_2 molar content at the inlet gas phase $y^i_{CO_2}$ (ppm)	9214	7740	2200	7740
DIC flow rate at the outlet ($mol{\cdot}L^{-1}{\cdot}h^{-1}$)	7.78×10^{-4}	6.41×10^{-4}	2.31×10^{-4}	5.94×10^{-4}
gas−liquid mass transfer coefficient k_La (h^{-1})	4.62	4.41	6.19	4.69
carbon gas−liquid transfer ($mol{\cdot}L^{-1}{\cdot}h^{-1}$)	7.55×10^{-4}	6.47×10^{-4}	2.18×10^{-4}	6.1×10^{-4}
CO_2 molar content at the outlet gas phase $y^o_{CO_2}$ (ppm)	4937	4075	964	4283
DIC concentration (M)	5.04×10^{-4}	1.33×10^{-4}	2.1×10^{-5}	5.8×10^{-4}
biomass productivity $\langle r'_x \rangle$ ($g{\cdot}L^{-1}{\cdot}h^{-1}$)	1.57×10^{-2}	1.36×10^{-2}	4.98×10^{-3}	1.25×10^{-2}
growth kinetic C-efficiency Γ (%)	1.0%	14.0%	65.0%	13.0%
simulation results	#1	#2	#3	#4
carbon gas−liquid transfer ($mol{\cdot}L^{-1}{\cdot}h^{-1}$)	7.55×10^{-4}	6.38×10^{-4}	2.19×10^{-4}	6.2×10^{-4}
CO_2 molar content at the outlet gas phase $y^o_{CO_2}$ (ppm)	5172	4123	955	4230
DIC concentration (M)	8×10^{-4}	2.35×10^{-4}	1.54×10^{-5}	5.5×10^{-4}
biomass productivity $\langle r'_x \rangle$ ($g{\cdot}L^{-1}{\cdot}h^{-1}$)	1.52×10^{-2}	1.4×10^{-2}	4.90×10^{-3}	1.36×10^{-2}
growth kinetic C-efficiency Γ (%)	3.6%	11.3%	66.0%	5.2%
prediction relative error (%)	#1	#2	#3	#4
DIC flow rate at the outlet	−8.2%	−0.5%	−5.3%	4.5%
carbon gas−liquid transfer	−5.5%	−1.5%	0.3%	1.5%
CO_2 molar content at the outlet gas phase $y^o_{CO_2}$	4.8%	1.2%	−0.9%	−1.2%
DIC concentration	90.5%	76.7%	−26.7%	−5.0%
biomass productivity $\langle r'_x \rangle$	−3.3%	2.7%	−1.6%	8.4%
growth kinetic C-efficiency Γ	593.7%	17.6%	1.1%	58.8%

[a]Experimental data were obtained for continuous cultures of *Chlorella vulgaris* grown with varying CO_2 concentrations in the injected gas at a constant PFD of 250 $\mu mol_{h\nu}{\cdot}m^{-2}{\cdot}s^{-1}$. Carbon fluxes transferred from the gas to the liquid phase and at the outflow of the PBR were obtained from online carbon analysis, enabling one to determine the gas−liquid mass transfer coefficient k_La (Le Gouic et al. 2021).[5] Growth kinetic C-efficiency·Γ·represents the yield between biomass productivity measured and biomass productivity obtained when carbon was provided in excess (i.e., $\langle r'_x \rangle = 1.6 \times 10^{-2}$ $g{\cdot}L^{-1}{\cdot}h^1$).

represent the various conditions of carbon and light limitations (and their possible coupling) that could be encountered in practice.

Model Validation on Carbon-Limited Cultures of *Chlorella vulgaris* in Lab-Scale Torus-Shaped PBR. The modeling allows predicting the influence of operating parameters such as (i) gas injection conditions (gas flow rate G and CO_2 content $y^i_{CO_2}$), (ii) medium feeding characteristics (DIC concentration in the feed, dilution rate D), (iii) gas−liquid mass transfer performances (gas−liquid mass transfer coefficient k_La), and (iv) growing culture conditions (photon flux density, depth of culture, volume of culture V_R, pH, and temperature). Predicted values (model outputs) are the CO_2 content in the gas outlet ($y^o_{CO_2}$) and the dissolved carbon concentration in the culture medium (C_T). Those predicted values allow determining all carbon fluxes involved in the process (see Section Modeling of Carbon Mass Transfer and of Carbon Growth Limitation).

The model was used to predict four operating conditions in the torus-shaped PBR, leading to different growth limitations by the carbon source (i.e., 1 to 65%). Results are given in Table 1. The model was found to be able to predict biomass productivities ($\langle r'_x \rangle$), the CO_2 content in the gas outlet ($y^o_{CO_2}$), and the various carbon fluxes with a very good accuracy (relative error < 10%). The larger errors were obtained on DIC concentration prediction, especially in the case of strong limitation by the carbon source (experiment #3). This can be explained by the low DIC value that tends to zero and then amplifies errors of prediction of the absolute value. But because of the Monod-type relation between the growth rate and DIC concentration, the impact on the growth rate remains moderate, allowing one to accurately predict biomass growth and then various fluxes, which was the main purpose of our model (error < 10% on biomass productivity).

Analysis of Carbon Fluxes Involved during *Chlorella vulgaris* Cultures in Lab-Scale Torus-Shaped PBR. Simulations were performed under various conditions of carbon supply for a detailed analysis of carbon fluxes involved during *Chlorella vulgaris* continuous culture in the torus-shaped PBR, here retained as a first case study. Other growth conditions were kept ($D = 0.0144$ h^{-1} and incident PFD of 250 $\mu mol_{h\nu}{\cdot}m^{-2}{\cdot}s^{-1}$, constant gas flow rate of 100 $mL{\cdot}min^{-1}$, and $k_La = 6.19$ h^{-1}). Results were expressed in terms of DIC concentration, CO_2 removal yield η (eq 8), and carbon biofixation rate $\langle r_{CO_2} \rangle$ (eq 6). Predictions were obtained as a function of the CO_2 molar fraction in the inlet gas phase $y^i_{CO_2}$ and for two feeding conditions, with and without carbon enrichment of the liquid phase injected here with a constant flow rate (i.e., carbon feeding rate equal to $\frac{C^i_T}{\tau_p}$, eq 4). For convenience, carbon transfer and biofixation rates were normalized with respect to the maximal carbon biofixation rate $\langle r_{CO_2,\,max} \rangle$ as obtained when only light limitation occurs (i.e., no carbon growth limitation; $\langle r'^{LL}_X \rangle$ as given in eq 9):

$$\langle r_{CO_2,max} \rangle = \langle r'^{LL}_X \rangle \frac{Y_{CO_2}}{M_{CO_2}} \tag{10}$$

Note that the normalized biofixation rate is similar to the yield Γ introduced previously to represent growth limitation (both growth and carbon biofixation being proportional). For the

https://doi.org/10.1021/acssuschemeng.2c03927
ACS Sustainable Chem. Eng. 2022, 10, 12826−12842

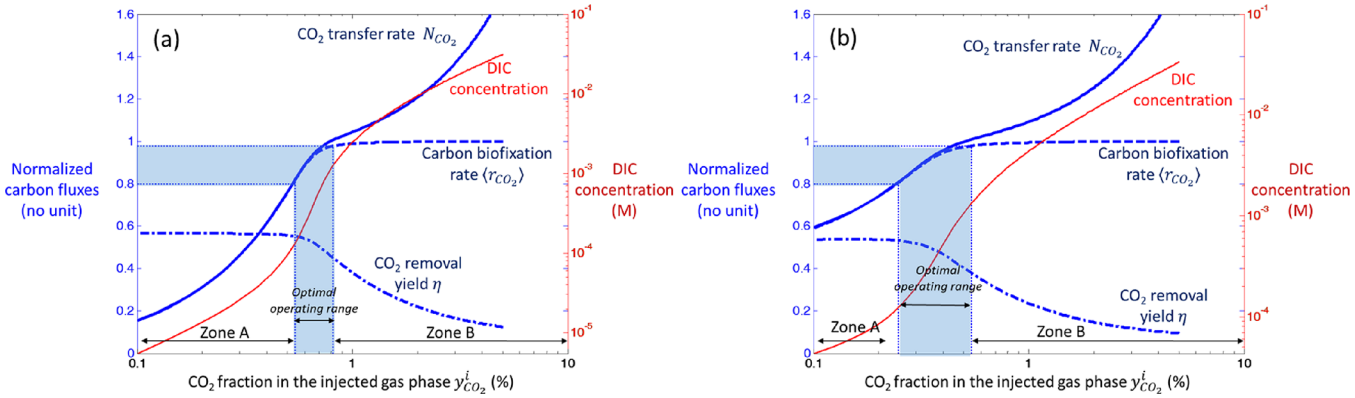

Figure 2. Simulations of the carbon fluxes involved in the torus-shaped PBR as a function of the CO_2 enrichment in the gas phase $y^i_{CO_2}$, namely, the CO_2 gas−liquid mass transfer rate N_{CO_2} (solid blue line) and the carbon biofixation rate $\langle r_{CO_2}\rangle$ (dashed blue line). The CO_2 removal yield η (dashdot blue line) and DIC concentration (solid red line) are also given. All fluxes are normalized by the maximum carbon biofixation rate $\langle r_{CO_2,\,max}\rangle$ as obtained in nonlimiting carbon limitation ($\langle r_{CO_2,\,max}\rangle = 6.5 \times 10^{-4}$ $mol_C \cdot L^{-1} \cdot h^{-1}$). Panels a and b give results without precarbonation of the culture medium in the feed and with 20 mM of DIC, respectively ($k_La = 6.19$ h^{-1}).

condition investigated here, $\langle r_{CO_2,\,max}\rangle = 6.5 \times 10^{-4}$ $mol_C \cdot L^{-1} \cdot h^{-1}$ and $\langle r'^{LL}_X\rangle = 1.65 \times 10^{-2}$ $g \cdot L^{-1} \cdot h^{-1}$.

Simulation #1: No Carbon Enrichment in the Feed. Prediction results with no prior carbon enrichment of the liquid phase are given in Figure 2a. The range of CO_2 molar fraction in the gas phase allows highlighting three different operating regimes:

- A regime (zone A) with an insufficient supply in CO_2 ($y^i_{CO_2}$<0.55%) with then growth limitation because of a DIC concentration below 0.1 mM. As a result, the carbon biofixation rate is below the maximal one, ranging from 18% at 0.1% in CO_2 in the gas phase to 80% at 0.55%. Because of the low DIC concentration, the CO_2 removal yield is maximal for the system considered (i.e., k_La value), i.e., around 58%.
- A regime (zone B) for values larger than 0.8% in CO_2, enabling photosynthetic growth that is not limited by the carbon source. The gas−liquid mass transfer N_{CO_2} is increasing with the increase in CO_2 fraction in the injected gas phase $y^i_{CO_2}$, but the carbon biofixation rate remains stable (growth is only limited by light, eq 10). Because of the increase in the pool of DIC with the CO_2 content in the gas phase, the CO_2 removal yield η drops progressively from 55% to below 20%.
- An optimal operating regime (between zones A and B) combining maximum productivity and an advantageous CO_2 content reduction in the gas phase. This regime corresponds to carbon biofixation rates close to maximal values, which were defined here arbitrarily as between 80 and 98% of the maximum biofixation rate $\langle r_{CO_2,\,max}\rangle$ (as fixed by eq 10). These operating conditions generate a DIC content in the culture medium of approximately 1 mM, allowing good gas−liquid mass transfer performance (i.e., large driving force) and then large CO_2 removal yield without leading to a significant drop in biomass productivity and then carbon biofixation rate. This optimal operating regime is obtained here for a CO_2 content between 0.5 and 0.9%, leading to a CO_2 removal yield between 58 and 40% (with then 42−60% of carbon loss in the gas outlet).

It can be noticed that, for zone A, the carbon biofixation rate $\langle r_{CO_2}\rangle$ is directly related to the transfer rate N_{CO_2} (curves are exactly superimposed). Because of the normalization of carbon fluxes with the maximum carbon biofixation rate $\langle r_{CO_2,\,max}\rangle$, a value close to 1 is obtained at the optimal range, indicating that the CO_2 transfer rate $N_{CO_2}$is equal to $\langle r_{CO_2,\,max}\rangle$ (in other words, all the CO_2 transfer is fixed by photosynthesis). Because of the growth limitation by light, increasing $y^i_{CO_2}$ leads to a gas−liquid mass transfer larger than carbon that can be biofixed, resulting then in DIC accumulation. As a direct consequence, CO_2 removal yield is maximal for a lower value of $y^i_{CO_2}$, as directly related to the ability to transfer CO_2 from the liquid to the gas phase (and consume it through photosynthetic growth). The same conclusion was observed in Le Gouic et al.[5] Such direct relation between physical (i.e., gas−liquid) and biological (i.e., photosynthesis) carbon fluxes could be generalized, and it was observed in all cases investigated.

In terms of culture operation, zone B will guarantee optimal biomass growth conditions with regard to carbon supply. Although less efficient with respect to CO_2 removal from the gas phase as when compared to zone A, it also guarantees a sufficient DIC buffer for a stable culture. In contrast, zone A would be of interest when aiming at optimizing CO_2 removal, but it would certainly be more challenging in terms of culture, as the limited amount of DIC may induce specific physiological responses such as carbon concentration mechanisms. As observed in Le Gouic et al.,[5] the decrease in growth rate will also reduce biomass concentration, increasing light-stress conditions with a concomitant pigment decrease, with a possible less stable growth.

Simulation #2: Carbon Enrichment in the Feed (20 mM). Carbon can be provided to the culture from the gas or liquid phase in the form of dissolved salts (i.e., carbonates). The contribution of the carbon source is then no longer only dependent on the gas−liquid mass transfer into the culture system. A 20 mM supply of carbon by the liquid phase was then simulated (Figure 2b).

By guaranteeing a minimum DIC in the liquid feed, the impact of the growth limitation by the CO_2 gas enrichment appears less marked. At 0.1% in CO_2, the carbon biofixation rate represents 18 and 60% of the maximum value without (simulation #1) and

https://doi.org/10.1021/acssuschemeng.2c03927
ACS Sustainable Chem. Eng. 2022, 10, 12826−12842

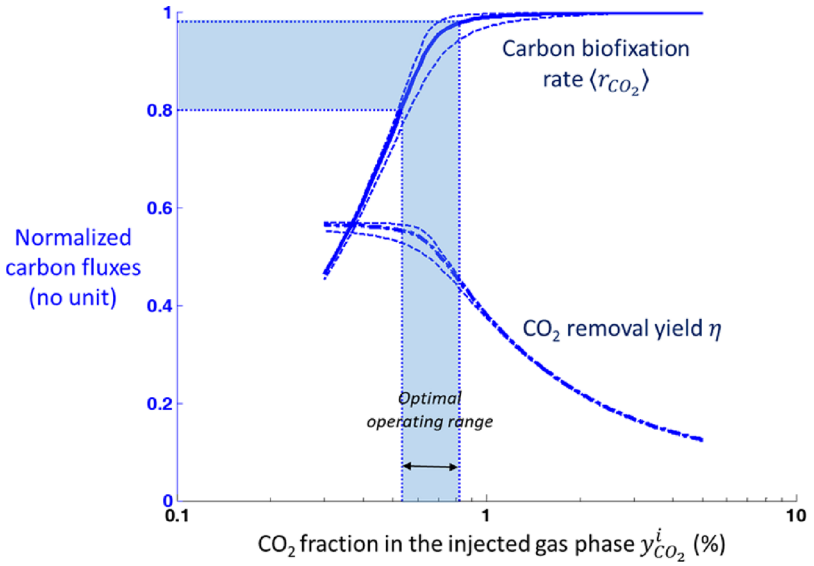

Figure 3. Sensitivity analysis of carbon flux prediction to the saturation constant value K_{DIC}. Same conditions of simulation #1 were applied (see Figure 2a). Predictions are here given for the carbon biofixation rate $\langle r_{CO_2} \rangle$ (solid blue line) and CO_2 removal yield η (dashdot blue line). Dashed lines give predictions for $K_{DIC}/3$ and $K_{DIC} \times 3$. All fluxes are normalized by the maximum carbon biofixation rate $\langle r_{CO_2,\,max} \rangle$ as obtained in nonlimiting carbon limitation ($\langle r_{CO_2,\,max} \rangle = 6.5 \times 10^{-4}$ $mol_C \cdot L^{-1} \cdot h^{-1}$).

with (simulation #2) carbon enrichment of the liquid phase, respectively. The feeding enrichment therefore makes it possible to offset the kinetic limitation by the carbon source. The three operating regimes observed previously are always obtained, but the CO_2 fractions in the gas phase are offset for about 0.3%: the optimal regime guaranteeing 80 to 98% of the maximum carbon biofixation rate is obtained for a molar fraction of CO_2 between 0.25 and 0.65%, with CO_2 removal yield between 0.35 and 0.55 (i.e., 0.55 corresponding to the maximal value obtained here).

As it should be, providing carbon from the liquid phase then requires a lower carbon concentration in the gas phase and reduces the risk of a carbon limitation because it is directly available to the algae cells. The maximum carbon biofixation rate is also reached more quickly. For a given value of CO_2 enrichment in the gas phase, the CO_2 removal yield is however reduced because of a lower gas−liquid mass transfer rate.

Sensitivity Analysis to the Saturation Constant K_{DIC}. The sensitivity of the model predictions to the saturation constant K_{DIC} value used in the kinetic modeling of the growth limitation by the carbon source was investigated. Results are given in Figure 3 and Table 2 for the same conditions of simulation #1 (same conclusions for other conditions, data not shown). Predictions were obtained for saturation constant K_{DIC} ranging from $K_{DIC}/3$ and $3K_{DIC}$ (with the reference value K_{DIC} = 0.033 mM) that were found to be good upper and lower bounds for the prediction of experimental growth rates (Figure 1).

Despite the large range of variation of K_{DIC} value (±300%), a moderate effect on the key quantities of the model's prediction is observed. Logically, the effect is more important in the range where the limitation by the carbon source appears. For nonlimiting values of carbon enrichment in the gas phase ($y^i_{CO_2}$ > 2% corresponding to C_T > 3 mM approximately) or, on the contrary, for a very low enrichment ($y^i_{CO_2}$ < 0.4% corresponding to C_T < 0.05 mM approximately), the difference is negligible. This is directly explained by the Monod-type formulation that tends toward 0 (i.e., no growth) or 1 (i.e., no growth limitation) for low DIC or nonlimiting DIC concentration. Predictions reveal sensitivity at the limit of growth limitation by the carbon source (the optimum operating range). Table 1 illustrates the influence on the prediction of this operating range by giving relevant values for its lower and upper boundaries (i.e., limits of zones A and B, corresponding to 80 and 98% of the maximum biofixation rate $\langle r_{CO_2,\,max} \rangle$, respectively). The most important effect is on the prediction of the DIC concentration C_T. Nevertheless, the influence on

Table 2. Sensitivity Analysis of Model Prediction to the Saturation Constant Value K_{DIC}[a]

value of saturation constant	$K_{DIC}/3$	K_{DIC} (reference value)	$K_{DIC} \times 3$
CO_2 removal yield η (80% of $\langle r_{CO_2,\,max} \rangle$)	56%	56%	52%
deviation with reference value of K_{DIC}	0%		7%
CO_2 enrichment of the gas phase $y^i_{CO_2}$ (at 80% of $\langle r_{CO_2,\,max} \rangle$) (in ppm)	5100	5125	5598
deviation with reference value of K_{DIC}	1%	NA	9%
DIC concentration C_T (at 80% of $\langle r_{CO_2,\,max} \rangle$, in mM)	0.055	0.1	0.343
deviation with reference value of K_{DIC}	45%	NA	243%
CO_2 removal yield η (98% of $\langle r_{CO_2,\,max} \rangle$)	50%	45%	32%
deviation with reference value of K_{DIC}	11%	NA	28%
CO_2 enrichment of the gas phase $y^i_{CO_2}$ (at 98% of $\langle r_{CO_2,\,max} \rangle$) (in ppm)	7251	8196	11,975
deviation with reference value of K_{DIC}	12%	NA	46%
DIC concentration C_T (at 98% of $\langle r_{CO_2,\,max} \rangle$, in mM)	0.65	1.3	3.8
deviation with reference value of K_{DIC}	50%	NA	192%

[a]Influence on the determination of the optimal operating range. Results are given at both boundaries of the optimal operating range (between 80 and 98% of the maximum biofixation rate $\langle r_{CO_2,\,max} \rangle$, see text for details) for various characteristic values, i.e., CO_2 removal yield η, CO_2 enrichment of the gas phase $y^i_{CO_2}$, and DIC concentration C_T. Same conditions of simulation #1 were applied (Figure 2a). The reference value of K_{DIC} is 0.033 mM.

https://doi.org/10.1021/acssuschemeng.2c03927
ACS Sustainable Chem. Eng. 2022, 10, 12826−12842

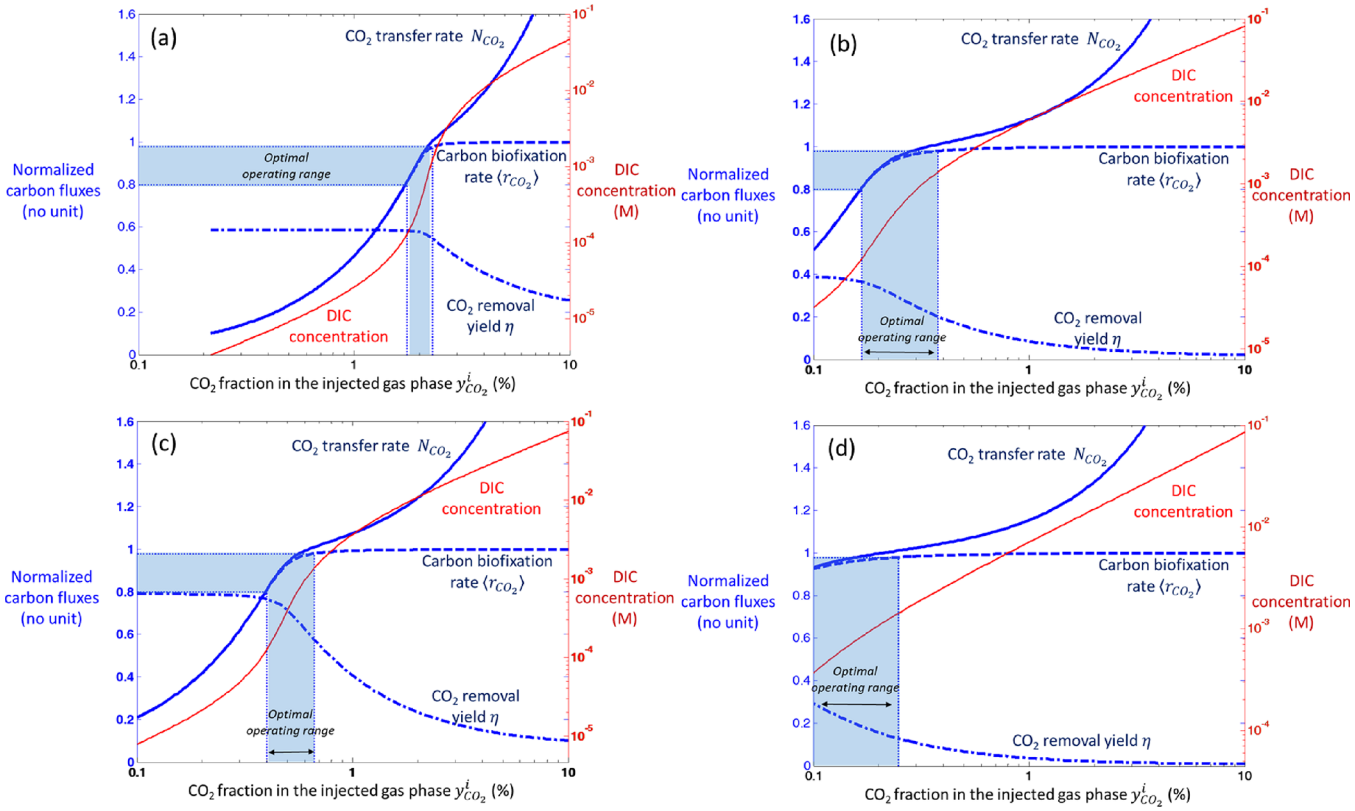

Figure 4. Simulations of the carbon fluxes involved in the torus-shaped (a: 0.02 vvm, $k_La = 1.13\ h^{-1}$; b: 0.04 vvm, $k_La = 9\ h^{-1}$) and in an airlift PBR (c: 0.02 vvm, $k_La = 8.75\ h^{-1}$; d: 0.8 vvm, $k_La = 80\ h^{-1}$) as a function of the CO_2 enrichment in the gas phase $y^i_{CO_2}$, namely, the CO_2 gas−liquid mass transfer rate N_{CO_2} (solid blue line) and the carbon biofixation rate $\langle r_{CO_2} \rangle$ (dashed blue line). The CO_2 removal yield η (dashdot blue line) and DIC concentration (solid red line) are also given. All fluxes are normalized by the maximum carbon biofixation rate $\langle r_{CO_2,\,max} \rangle$ as obtained in nonlimiting carbon limitation ($\langle r_{CO_2,\,max} \rangle = 6.5 \times 10^{-4}\ mol_C \cdot L^{-1} \cdot h^{-1}$). All simulations were conducted without precarbonation of the culture medium in the feed.

relevant values characterizing the efficiency of the process, namely, CO_2 removal yield η and corresponding CO_2 enrichment of the gas phase $y^i_{CO_2}$, is low. A difference of less than 10% is obtained for the lower limit (80% of $\langle r_{CO_2,\,max} \rangle$). A higher deviation is obtained for the upper limit (98% of $\langle r_{CO_2,\,max} \rangle$), explained here by the asymptotic nature of the evolutions when the carbon supply reaches nonlimiting values.

Illustrations for the Optimization of the Carbon Feeding Strategy in Microalgal Culture Systems. *Lab-Scale Photobioreactors. Introduction.* As another illustration of the use of our model, two lab-scale PBRs were simulated to illustrate the role of the mixing and aeration conditions on the CO_2 use efficiency, namely, conventional airlift PBR in addition to the torus-shaped PBR previously described (Figure 5). The aim was to illustrate the influence of mechanical agitation (i.e., the torus-shaped PBR is mixed by a marine impeller coupled with a co-current injection of a gas containing a molar fraction of CO_2 at a variable flow rate) with standard aeration of airlift PBRs that are usually used in algae culture.

Because of the mechanical agitation, the gas flow rate in torus-shaped PBR can be adjusted from low (i.e., around 0.01 vvm) to large values (i.e., around 0.8 vvm).[20,21] For airlift PBR, the gaseous supply is used for both homogenization of the algal suspension and gas−liquid mass transfer (i.e., gas enriched in CO_2). Usually, larger flow rates of around 0.05−1 vvm are applied to obtain good cell suspension conditions.[22,23]

Simulations were conducted for two typical operating conditions for each PBR (same culture volume of 1.45 L): a low and high gas flow rate. Values of k_La were obtained from Loubiere et al.[22] for the airlift PBR (i.e., vertical tubular PBR) and Kazbar et al.[20] for the torus-shaped PBR. For comparison, the same value of low gas flow rate was considered for both geometries (0.02 vvm), leading to k_La values of around 1.93 and 8.75 h^{-1} for mechanically and airlift stirred PBRs, respectively. We can note here the better gas−liquid mass transfer performance of airlift PBR for similar gas flow rates. To investigate the upper limit of the torus-shaped PBR in terms of gas−liquid mass transfer, a gas flow rate of 0.4 vvm was simulated (k_La = 15.35 h^{-1}), corresponding roughly to the maximal value that could be applied in practice in such a system (flow rate of 580 mL/min for a total culture volume of 1.3 L). For the airlift PBR, a flow rate of 0.8 vvm was applied, with such value enabling one to obtain a large k_La value of 80 h^{-1} (5 times higher for half the flow rate applied in the torus-shaped PBR).

Simulation Results. In the case of the torus-shaped PBR with a low gas flow rate of 0.02 vvm (Figure 4a), a minimum fraction of CO_2 in the gas phase of 0.2% is necessary to bring enough carbon to the liquid phase to allow a non-null DIC content. Optimal operating performance is obtained for a CO_2 molar fraction of approximately 2%, with larger values then enabling nonlimiting growth by the carbon source. The maximal CO_2 removal yield is 58%.When increasing the gas flow rate (Figure 4b), the CO_2 molar fraction required to obtain optimal growth conditions decreases (around 0.2−0.3%), as does the CO_2

https://doi.org/10.1021/acssuschemeng.2c03927
ACS Sustainable Chem. Eng. 2022, 10, 12826−12842

removal yield (maximal value 40%). We can note a significant decrease in CO_2 removal yield if a high flow rate is combined with high CO_2 enrichment. For example, if a 2% enrichment is applied (the optimal regime for the flow rate of 0.02 vvm), a CO_2 removal yield of 5% is obtained (compared to 58% for 0.02 vvm). This illustrates the strong relation between flow rate and CO_2 enrichment in the gas phase.

Airlift PBR shows a similar evolution with the increase in gas flow rate but with different values. Because of a better gas−liquid mass transfer efficiency, the optimal operating condition obtained for the low gas flow rate (Figure 4c) requires a CO_2 fraction of 0.4−0.7% (2% for the torus-shaped PBR, same flow rate), with a CO_2 removal yield of up to 80% (58% for the torus-shaped PBR). For the high flow rate (Figure 4d), a CO_2 enrichment of 0.25% is sufficient to obtain growth conditions not limited by the carbon but with a significant decrease in CO_2 removal yield (<30%). As a drawback of the larger gas−liquid mass transfer efficiency of the airlift PBR, we can note also a stronger decrease in CO_2 removal yield when increasing the CO_2 fraction in the gas phase. For example, for a 2% enrichment, the CO_2 removal yield decreased below 1% for the largest flow rate.

Discussion on the CO_2 Use in Mechanically Stirred and Airlift Culture Systems. Those results illustrate the wide range of CO_2 removal yield that could be covered depending of PBR geometry, gas flow rate, and CO_2 enrichment. With a tight optimization (i.e., working at the optimal regime), CO_2 removal yields up to 80% were obtained here, with however a rapid drop when increasing the CO_2 enrichment or gas flow rate. This is especially the case for airlift PBR that presents better gas−liquid mass transfer, with then a more sensitive relation to operating parameters: a CO_2 removal yield below 1% was obtained when large CO_2 enrichment is combined with large flow rate. A direct consequence would be the increase of the operating cost due to CO_2 feeding. More than 99% of the injected CO_2 will indeed be lost at the PBR outlet, while working at optimal operating conditions would produce the same amount of biomass (as only fixed by the light supply), then saving a significant amount of CO_2. It must be recalled that the setting of the gas flow rate in airlift PBR is not only a question of gas−liquid mass transfer but also a question of mixing for cell suspensions as well as promoting light−dark cycles.[24−26] Therefore, large flow rate values are often applied in practice, with then low CO_2 removal yields. Regarding our results, a value below 10% can be guessed for an airlift PBR technology.

In terms of practical consequences in the context of microalgal biomass production (and then CO_2 biofixation), it must be added that nonlimiting growth conditions by the carbon source were more easily obtained with airlift PBR: according to our prediction, only a slight CO_2 enrichment (<1%) was indeed found sufficient to reach enough DIC concentration. If the purpose is to maximize biomass production (independently of the cost of CO_2 supply or CO_2 removal yield), airlift PBR will be therefore easier to operate, explaining certainly why such a technology is widely used in the field. Our results however emphasize that a significant amount of CO_2 could be saved with a proper optimization (around 30−40% of CO_2 removal yield, to be compared to a few percent when using a gas rich in CO_2).

Covered Raceways for Industrial-Scale Production. Introduction. The use of our model was extended to the case of a raceway system as another example of a mechanically stirred culture system (i.e., paddle wheel mixing) that is widely used for large-scale culture of photosynthetic microorganisms. Unless very strong basic conditions are applied, the CO_2 molar fraction of the atmosphere is insufficient to provide optimal growth of photosynthetic microorganisms. A supply of carbon is therefore often carried out either by addition in the form of carbonated chemical species previously dissolved or by bubbling a gas phase enriched in CO_2.

As an alternative to the classic principle of raceway design (i.e., open system), establishing a controlled atmosphere above the gas−liquid interface can be useful to increase the DIC concentration in the culture.[14] This can be obtained in practice by covering the raceway with a transparent cover, allowing imposing a CO_2 molar fraction greater than that of the atmosphere at the gas−liquid interface (which is roughly equal to almost the ground surface occupied by the raceway).

The following example assesses the potential of this technology hereafter named covered raceway (Figure 5) as a culture system to produce microalgal biomass (when compared to an open system).

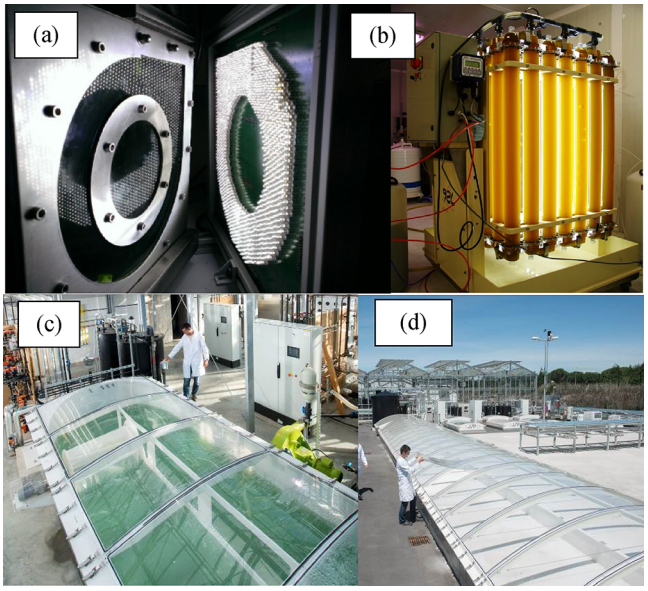

Figure 5. Torus-shaped PBR for (a) lab-scale investigations, (b) airlift tubular PBR, and (c, d) covered raceway for outdoor culture.

Simulated Conditions. The principle of a covered raceway system allows using the same model as described for the torus-shaped PBR (i.e., closed system) with a CO_2 content in the controlled atmosphere that could be greater than the natural value in atmosphere. The CO_2 content is then the result of the gas−liquid mass transfer and carbon biological assimilation in the culture system.

The gas−liquid mass transfer of a raceway culture system is known to be low because it depends mainly on the exchange that takes place at the gas−liquid interface, which is only influenced by mixing induced by the paddle wheel.[20,27] Weissman et al.[27] gave a k_La value of 0.5 h^{-1}, which will be retained here. Simulations will be conducted by arbitrarily choosing an illuminated surface of 100 m^2 per culture system with a depth of culture of 0.2 m (i.e., culture volume of 20 m^3). An aeration flow rate of 0.025 vvm (i.e., 250 $L{\cdot}min^{-1}$ for a 100 m^2 raceway system of 0.2 m of culture depth) will be applied (data obtained on covered raceways used in our facility, data not shown).

Each simulation uses the same culture conditions as in the previous section (*Chlorella vulgaris*, PFD of 250 $\mu mol_{hv}{\cdot}m^{-2}{\cdot}s^{-1}$,

https://doi.org/10.1021/acssuschemeng.2c03927
ACS Sustainable Chem. Eng. 2022, 10, 12826−12842

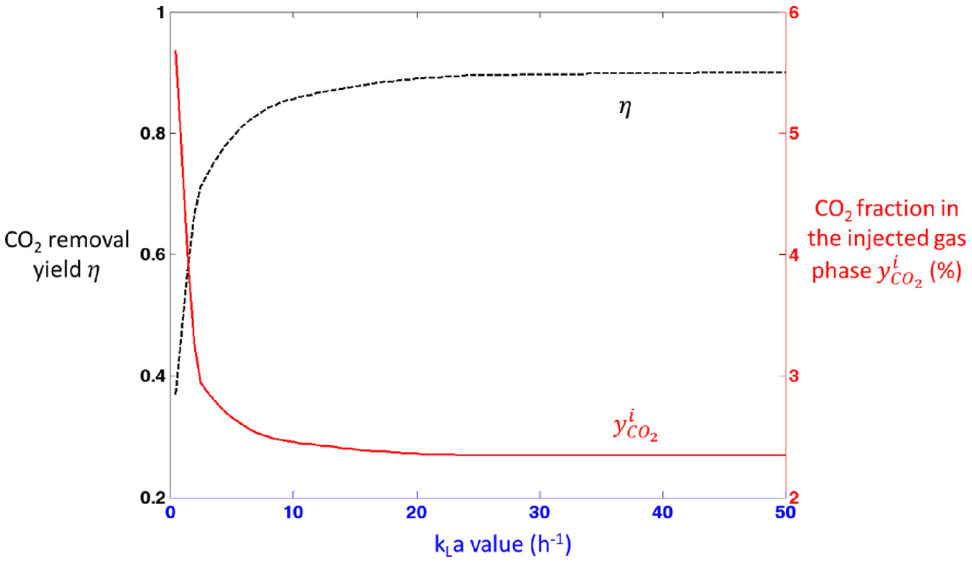

Figure 6. Investigation of the interest of a covered raceway to produce microalgal biomass with optimal use of injected CO_2. The influence of the gas−liquid mass transfer performance (k_La value) on the CO_2 enrichment in the gas phase $y^i_{CO_2}$ needed to obtain optimal operating conditions (i.e., 98% of maximal biomass production) is given, with the corresponding CO_2 removal yield. All simulations were conducted without precarbonation of the culture medium in the feed.

pH at 7.5, culture temperature of 25 ° C, and residence time of 70 h). Biomass volumetric productivity was determined by considering the areal productivity (i.e., S_X = 15.4 g·m^{-2}·day^{-1}) constant whatever the culture depth,[13,28] leading to volumetric productivity $P_X = 3.2 \times 10^{-3}$ g·L^{-1}·h^{-1} for a raceway of 0.2 m depth.

It must be noticed that solar conditions were not simulated to simplify the discussion. However, our growth model was already proven to be valid to simulate the solar culture for various locations and periods of the year.[29,30] Similarly, Le Gouic et al.[5] demonstrated the ability of the CO_2 dissolution model for varying pH conditions. The modeling approach could then be extended if needed with limited effort to those cases to simulate more realistic conditions.

Influence of the Gas−Liquid Mass Transfer (k_La) in Covered Raceway Systems. As demonstrated previously, an optimal operating range in carbon feeding can be determined, corresponding to the minimum CO_2 enrichment needed in the injected gas phase to provide sufficient carbon to avoid carbon growth, while avoiding impairment of the gas−liquid mass transfer with a too large DIC accumulation in the liquid phase. Such a condition could be considered as the best compromise between CO_2 biofixation (i.e., 80−98% of the maximum biofixation) and CO_2 removal yield.

The model predicted that such operating range was obtained for a covered raceway with standard performance in gas−liquid mass transfer (k_La = 0.5 h^{-1}) for a CO_2 enrichment of 5.7%, leading to a maximal CO_2 removal yield of 37%. Otherwise, a minimum of around two-thirds of CO_2 injected in the culture system is then lost in the gas outlet.

As shown previously when comparing airlift and torus-shaped PBR, by improving the k_La value, the carbon flux transferred to the liquid phase can be improved, which will also modify the CO_2 removal yield. In terms of engineering, it can be obtained in raceway systems (open or closed) by improving gas injection through an optimized injection device with, for example, microbubbles or by applying multiple injection locations in the culture system. Simulations were then conducted to define to what extent it would be interesting to improve the mass transfer of a covered raceway subjected to the bubbling of a gas enriched in CO_2 as a means to increase the gas−liquid mass transfer performance of the system. Similarly to the previous simulations, the aim was to determine for which operating conditions was the carbon biofixation equal to 98% of the maximum biofixation (i.e., no carbon limitation). In addition to a variation in CO_2 enrichment of the gas phase ($y^i_{CO_2}$), the gas−liquid mass transfer (k_La) was varied. Predicted results are given in Figure 6.

As already noticed, the k_La value of a standard raceway (k_La = 0.5 h^{-1}, the lowest simulated value in Figure 6) requires a gas supply with at least 5.7% enrichment in CO_2 to bring enough carbon to the culture. Under these conditions, CO_2 removal yield is less than 40%. By increasing the k_La value by a factor of 5 (k_La = 2.5 h^{-1}), CO_2 removal yield reaches about 70% for the same biomass productivity and then carbon biofixation. In fact, the necessary CO_2 concentration ($y^i_{CO_2}$) is lower because almost all of the injected carbon is transferred to the liquid phase and therefore used by the microalgal biomass. The improvement of gas−liquid mass transfer (i.e., k_La value) of the covered raceway allows obtaining CO_2 removal yields greater than 80% (k_La > 10 h^{-1}) for CO_2 contents between 2 and 3% in the gas phase. However, this requires a significant improvement in the gas−liquid transfer (factor of 20 compared to the value of 0.5 h^{-1} as reported in the literature). It could be obtained through optimized gas injection (as shown previously, values greater than 10 h^{-1} were obtained for both torus-shaped and airlift PBR). Those results tend to emphasize the interest of the covered raceway in the context of CO_2 valorization: assuming an improved (but realistic) gas−liquid mass transfer performance, CO_2 removal yields of up to 80% can be reached (to be compared to the maximal value of 30−40% obtained for the airlift PBR).

Interest of a Precarbonation. As discussed previously, carbon can be supplied through precarbonation of the liquid phase in addition to the enrichment of the gas phase (dissolution of carbonate salts for example). It avoids the gas−liquid mass

https://doi.org/10.1021/acssuschemeng.2c03927
ACS Sustainable Chem. Eng. 2022, 10, 12826−12842

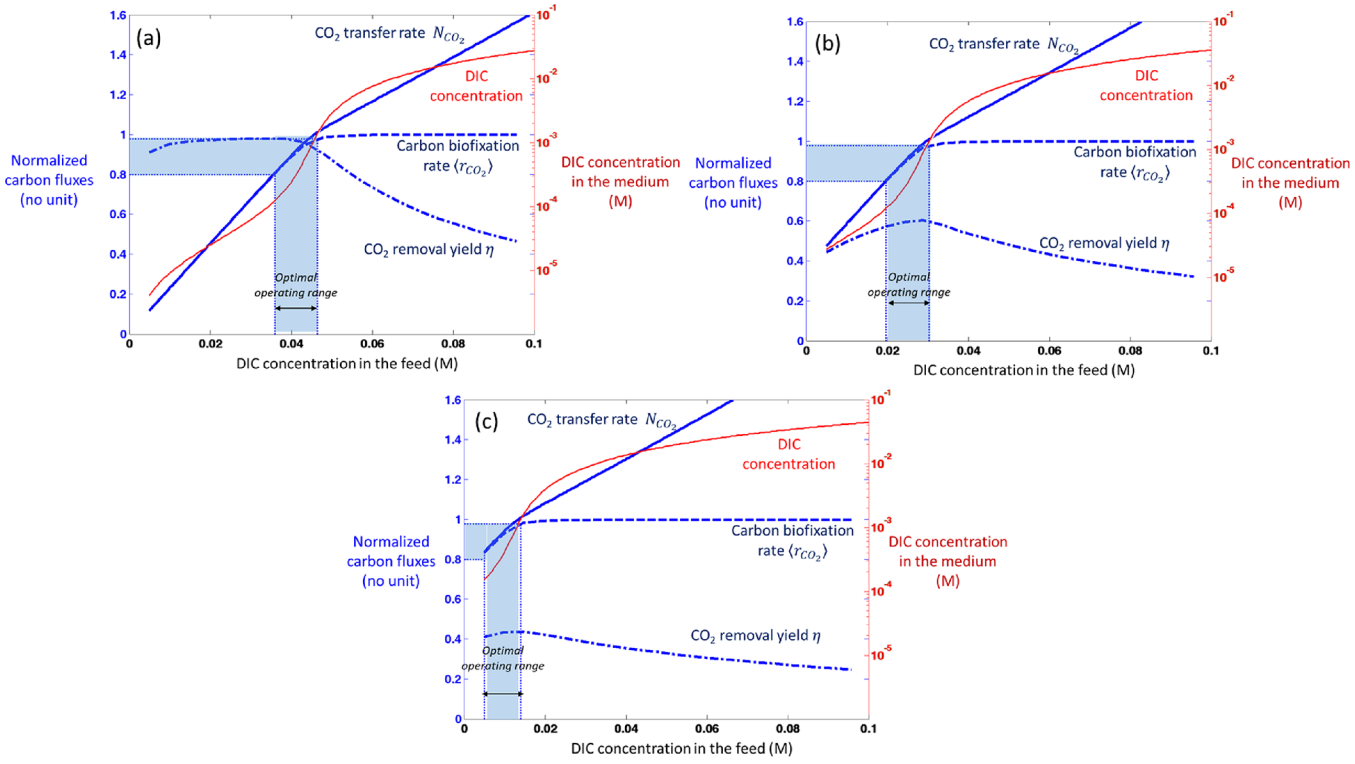

Figure 7. Investigation of precarbonation of the culture medium in the feed for a raceway of 100 m^2 (k_La value of 0.5 h^{-1}, aeration flow rate of 0.025 vvm, total volume of 20m^3). Carbon fluxes and DIC concentration in the culture system are given as a function of the DIC concentration in the feed. Panel a shows an open system fed with air (i.e., 0.38% in CO_2), and panels b and c show a covered raceway fed with a CO_2 enriched gas of 2 and 4%, respectively. The CO_2 gas−liquid mass transfer rate N_{CO_2} (solid blue line), carbon biofixation rate $\langle r_{CO_2} \rangle$ (dashed blue line), CO_2 removal yield η (dashdot blue line), and DIC concentration (solid red line) are given. All fluxes are normalized by the maximum carbon biofixation rate $\langle r_{CO_2,\,max} \rangle$ as obtained in nonlimiting carbon limitation ($\langle r_{CO_2,\,max} \rangle = 1.3 \times 10^{-4}$ $mol_C \cdot L^{-1} \cdot h^{-1}$).

transfer limitation of the raceway culture system. As an additional advantage when associated to a covered culture system, carbon desorption phenomena will be limited by the enrichment of culture system gas phase, contrary to the open system where CO_2 desorption can occur due to the low atmosphere content in CO_2 of around 0.38−0.5%.

To investigate the interest of precarbonation with covered raceways, three different CO_2 fractions were imposed as a gas atmosphere, namely, 0.38, 2, and 4% CO_2. The same raceway was considered (surface of 100 m^2, k_La = 0.5 h^{-1}, and gas flow rate of 250 $L \cdot min^{-1}$). The value of 0.38% was used here to represent an open raceway in contact with the atmosphere. Simulations were then conducted as a function of the DIC concentration of the feed.

The effect of a prior dissolution through precarbonation is here shown when cultivating algae in an open raceway (Figure 7a). A CO_2 removal yield η of almost 100% for a DIC injection between 0 and 40 mM is found. Under these conditions, all the carbon supplied in dissolved form is consumed by the photosynthetic growth. However, we can notice that if the DIC concentration in the feed is below 35 mM, the carbon biofixation rate is less than 80% of the maximum value with a lower possible value of 10%, which indicates insufficient carbon input to obtain optimal growth. The DIC concentration in culture remains indeed almost null until the DIC concentration in the precarbonated feed becomes greater than 40 mM. Beyond this value, the biofixation rate becomes the maximum, which testifies to a growth not limited by the carbon source. Consequently, part of the injected carbon is then found in dissolved form, causing a drop in the carbon removal yield simultaneous to the progressive increase in DIC concentration in the medium (i.e., decrease of CO_2 dissolution in the liquid phase).

The establishment of a controlled atmosphere composed of 2% CO_2 (Figure 7b) leads to a decrease in the CO_2 removal yield, with a maximum value less than 60%. Combination of a CO_2 enrichment with precarbonation increases the loss of CO_2 at the culture system outlet. However, this strategy enables one to reduce the DIC concentration needed in the feeding medium. In addition, while in an open system we could observe very strong limitations of growth by the carbon source (only 20% of the maximum biofixation rate for DIC = 10 mM, Figure 7a), a 2% CO_2 enrichment of the gas phase guarantees growth, ensuring a biofixation rate greater than 40% of the maximal permitted value whatever the condition.

By observing the results in more detail, it can be observed that, by creating a CO_2 enrichment in the culture system atmosphere, carbon desorption remains limited, allowing less carbon to be added in the feed to obtain the same DIC concentration in the culture. It is shown when considering a given DIC concentration in the feed: the DIC concentration in the medium is larger when using the covered raceway due to CO_2 enrichment of the gas phase. The CO_2 removal yield is nevertheless lower due to the higher losses at the culture system outlet.

The same conclusions are obtained for a gaseous atmosphere containing 4% CO_2 (Figure 7c). The CO_2 removal yield decreases further (maximum barely greater than 40%), but it nevertheless appears that, even without an external carbon

https://doi.org/10.1021/acssuschemeng.2c03927
ACS Sustainable Chem. Eng. 2022, 10, 12826−12842

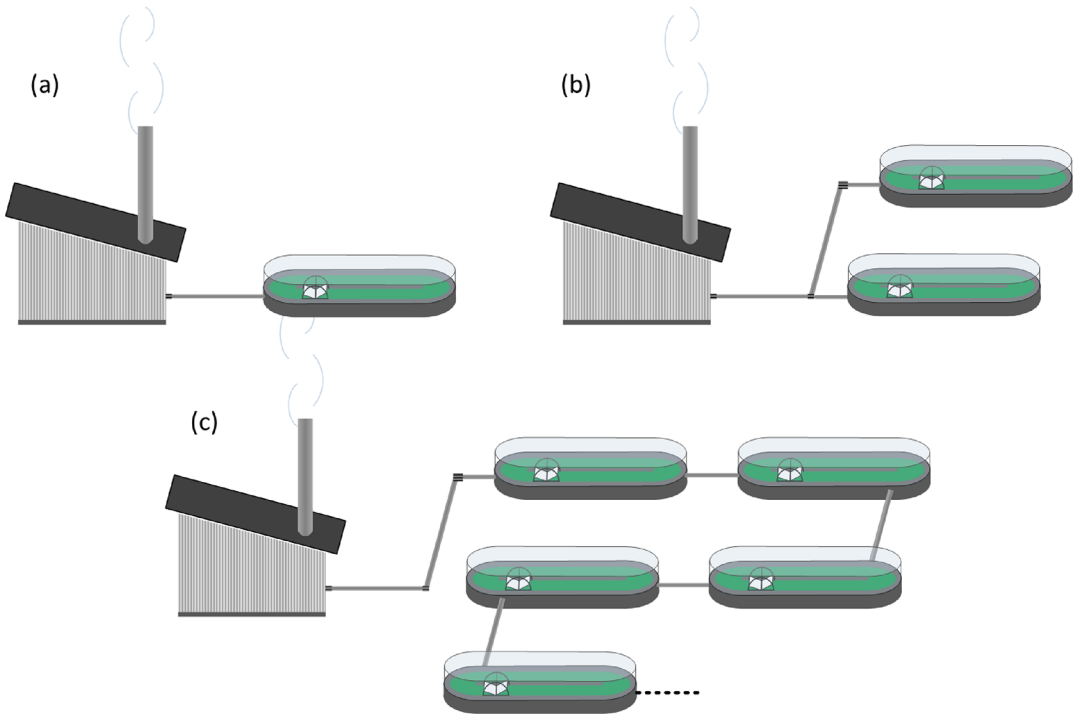

Figure 8. Configurations of culture systems simulated: (a) single system, (b) multistage system in parallel, and (c) multistage system in series.

supply, the carbon biofixation rate is at least equal to 80% of the maximum one: when using an enrichment of 4% in CO_2, growth will never be severely limited by the carbon source. Adding 13 mM of DIC is enough to reach maximal growth performance (and then carbon biofixation rate).

Discussion on the Relevance of the Covered Raceway Technology on CO_2 Use. Previous results allow drawing some general conclusions regarding the relevance of the covered raceway with regard to CO_2 supply and use:

- Without precarbonation, an injection of a gas enriched at least in 5.7% in CO_2 is needed in a covered raceway to reach nonlimiting growth condition for a usual k_La value of 0.5 h^{-1}. However, it also corresponds to a low carbon removal yield (below 40%). Gas−liquid mass transfer is of primary relevance here, as it directly affects the removal yield (a value of 80% was achieved for k_La = 10 h^{-1}).
- When using precarbonation, the DIC concentration in the feed necessary to achieve a nonlimiting value will be lower for larger CO_2 enrichment of the gas phase. Consequently, a covered raceway by creating a gaseous atmosphere different from the ambient is of interest here: it needs a lower DIC concentration compared to open systems (at least 40 mM enrichment compared to 25 and 10 mM for a covered raceway supplied in 2 and 4% in CO_2 in the gas phase, respectively).
- The more the gaseous atmosphere will be enriched in CO_2, the lower the CO_2 removal will be (more loss at the reactor outflow). Thus, for an atmosphere composed of 4% CO_2 in a closed raceway, the maximal value is around 40% compared to 98% for an open system. Increasing gas−liquid mass transfer of the culture system will enable the increase in CO_2 removal while allowing one to work with a lower CO_2 enrichment in the injected gas phase.
- By allowing to keep a gas phase enriched in CO_2, the covered raceway has better performance in CO_2 removal yield when compared to airlift technology: up to 80% can be reached for a maximal value of 30−40% in airlift PBR (with usual estimated values below 10%).

Numerical Investigation of Various Strategies for a Typical Flue Gas (16% in CO_2). *Introduction.* As a final illustration of the practical interest of our model, simulations were extended to the case of CO_2 emitted from flue-gas.[1,7,8,31−33] Obviously, exact simulation should support further adaptation of our model, like the integration of day−night cycles as such application would require mass-scale production and then sunlight use. But the purpose here was just to illustrate the interest of our model to predict key values such as CO_2 removal yield and biomass production as a function of engineering values like the surface of culture and various supply configurations such as multistage configuration of culture systems.

A CO_2 molar content of 16% was here retained as a case study, representative of the one obtained from flue gas from the cement factories for example (data obtained from an industrial partner). Such value is of interest because it is significantly different from conditions usually encountered at the lab scale, where either small CO_2 enrichment (1−2%) or, in contrast, pure CO_2 controlled by pH regulation is used.

A 16% enrichment makes it possible to reach at gas−liquid phase equilibrium a theoretical concentration of DIC of around 80 mM, perfectly compatible with good growth conditions of the biomass without any limitation per the carbon source (which occurred below around 1 mM, as shown previously). Consequently, the biological fixation will be maximal (i.e., as fixed by photosynthetic growth). The driving force imposed by a 16% content in the gas phase will also be sufficiently high to partly compensate the low gas−liquid mass transfer performance of the culture system. The main drawback here is in the CO_2 abatement in the gas phase. As also shown previously, because of the large content of the CO_2 in the gas phase, CO_2 removal yield will decrease quickly, and the majority of the injected CO_2 will be found at the reactor outlet.

https://doi.org/10.1021/acssuschemeng.2c03927
ACS Sustainable Chem. Eng. 2022, 10, 12826−12842

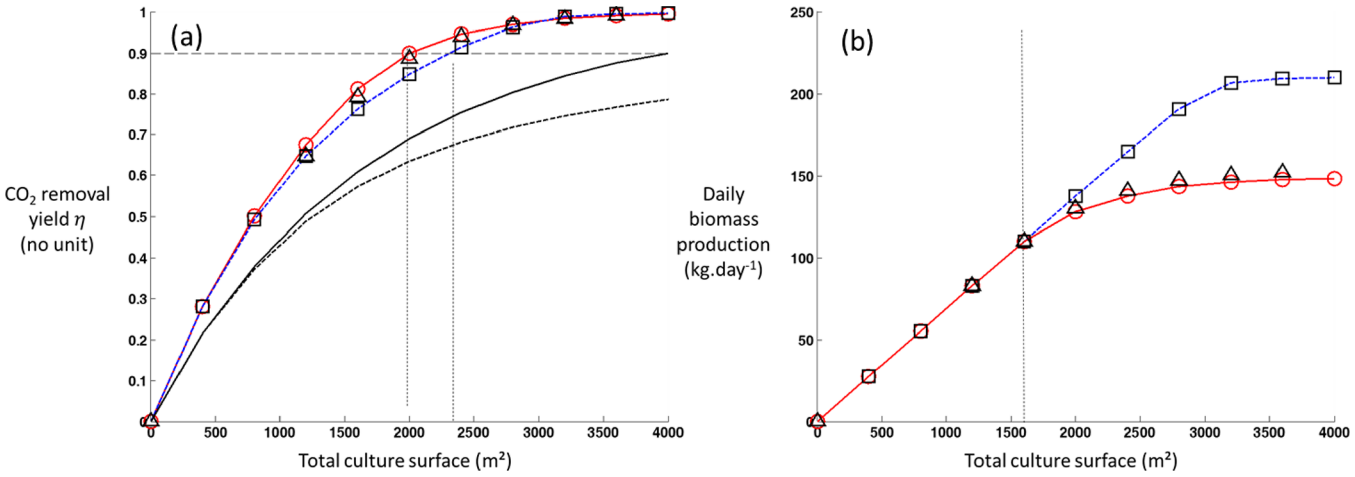

Figure 9. Investigation of various configurations for CO_2 valorization of a gas containing 16% in CO_2 typical of a flue gas (flow rate of 1000 L·min^{-1}). (a) CO_2 removal yield and (b) daily biomass production are given as a function of the total culture system for a single system (dashed blue line) and a multistage system composed of a covered raceway connected in series (solid red line) and in parallel (black square). CO_2 removal yields for systems without biological fixation (i.e., no algae) are given (solid black line for a multistage system in series; dashed black line for a single system). For the multistage system, a covered raceway of 400 m^2 was considered (k_La value of 0.5 h^{-1}, aeration flow rate of 0.025 vvm, and total volume of 80 m^3). A combination of a large culture system (1200 m^2) followed by a multistage system in series is given (black triangles). All simulations were conducted without precarbonation of the culture medium in the feed.

As usually applied in chemical engineering, for example, in absorption processes,[34] the principle of multistage reactors can be of interest here. When using covered systems (such as covered raceways, as used previously), the gaseous effluent can be injected in a first culture system and then connected in series with several others, forming a multistage cultivation system (Figure 8c). The effluent from one culture system is simply obtained from its gas phase, which is injected in the following culture system. The highly concentrated CO_2 gas will be progressively depleted as it changes from stage to stage. As an alternative to multistage reactors connected in series, parallel feeding in a single unit can also be considered (Figure 8b). The interest is that the total gas flow rate is divided on each culture system, reducing the amount of CO_2 (but not the gas content) provided to each culture system.

To illustrate the potential of our model to investigate various feeding strategies, four configurations were simulated:

- a usual configuration with a single system (i.e., reference scenario) with the same cumulated area and volume of the multistage system (simulation A),
- a multistage system composed of a similar culture system (area of 400 m^2 and volume of 80 m^3) connected in series (simulation B),
- a multistage system composed of a similar culture system (area of 400 m^2 and volume of 80m^3) connected in parallel (simulation C), and
- a multistage system combining culture systems of different surfaces (simulation D).

The same gas supply (1000 L·min^{-1}, 16% in CO_2) and gas−liquid performances (k_La = 0.5 h^{-1}) were considered for all scenarios.

Simulation Results. Analysis of Global Performances. Single-stage (simulation A) vs multistage culture system connected in series (simulation B): Figure 9 gives the CO_2 removal yield η (Figure 9a) and daily biomass production (Figure 9b) as a function of total culture surface involved for each of the three configurations investigated (i.e., surface of the single system; cumulated surface for multistage systems). Those two quantities, CO_2 removal yield η and daily total biomass production, were retained as key values in the perspective of finding a compromise between cleaning a flue gas from its CO_2 content before its emission in atmosphere, with the aim of maximizing the microalgal biomass production for further valorization. As shown before, such a compromise is not straightforward, as a low CO_2 content would result in growth limitation by DIC concentration.

As expected, the multistage system connected in series leads to different performances in both CO_2 removal yield and daily biomass production. Regarding CO_2 removal yield, a better efficiency is obtained for surfaces between 800 (two stages) and 2800 m^2 (seven stages). For example, a target of 90% CO_2 removal would be obtained with 2400 and 2000 m^2 for a single system and a multistage system connected in series, respectively. For lower and higher surfaces, the CO_2 removal yield was found to be almost identical for a given surface. Those results were expected: for lower surfaces, a minimum surface is required for a sufficient decrease in CO_2 gas content of the rich flue gas (16%); for larger surfaces, the difference between configurations decreases when approaching the asymptotic limit of 100% of CO_2 removal yield (such results will be explained more deeply in the analysis per stage given in the next section).

Regarding daily biomass production, differences were observed for surfaces larger than 1600 m^2 (four stages in the multistage system), with a larger biomass production for the single system, increasing up to around 210 kg·day^{-1} obtained from 3600 m^2 corresponding to an almost full fixation of emitted CO_2 into biomass (also corresponding to almost 100% CO_2 removal efficiency, Figure 9a). For the multistage system in series, the maximal daily biomass production was reached more quickly for surfaces larger than 1600 m^2, reaching around 150 kg·day^{-1}, 28% lower than with the single system (this difference in algae production capacity will be explained later).

Performance of a parallel arrangement in a multistage culture system (simulation C): Figure 9 gives results for the multistage system in parallel (i.e., black square). Similar results were obtained as with the single system on both CO_2 removal yield and daily biomass production. Such a result could be considered

https://doi.org/10.1021/acssuschemeng.2c03927
ACS Sustainable Chem. Eng. 2022, 10, 12826−12842

Table 3. Detailed Analysis of the Influence of the Surface of the Different Configurations on DIC Concentration, CO_2 Content in the Gas Outflow, and Carbon Biofixation Rate

	total surface of culture	400 m^2	800 m^2	1200 m^2	2400 m^2	3200 m^2	4000 m^2
single system and multistage system in parallel (same results)	DIC concentration (mM)	51.6	39.7	29.4	7.7	0.4	0.1
	CO_2 content in the outflow ($y^o_{CO_2}$)	11.5%	8%	5.6%	1.4%	0.2%	0.05%
	normalized carbon biofixation rate	99.9%	99.9%	99.9%	99.6%	93.7%	76%
multistage system in series	DIC concentration (mM)	51.6	30.8	15	<0.01	<0.01	<0.01
	CO_2 content in the outflow ($y^o_{CO_2}$)	11.5%	8%	5.2%	0.9%	0.2%	0.1%
	normalized carbon biofixation rate	99.9%	99.9%	99.8%	83.3%	66.2%	53.8%

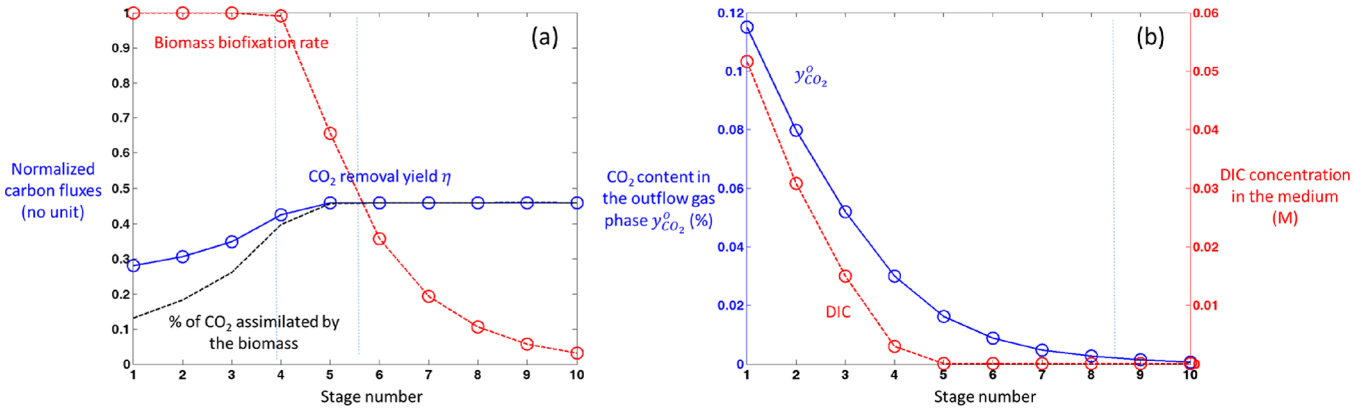

Figure 10. Detailed analysis of the multistage system in series for CO_2 valorization of a gas containing 16% in CO_2 typical of a flue gas (flow rate of 1000 $L{\cdot}min^{-1}$). (a) CO_2 removal yield, biomass biofixation rate, and % of CO_2 assimilated by the biomass and (b) DIC concentration and CO_2 content in the gas outflow are given as a function of stage number (i.e., covered raceway of 400 m^2).

surprising, but it is simply explained by the fact that the flow rate and thus CO_2 feeding are divided over the number of culture systems. As a result, each culture system behaves like a single unit fed with a lower gas and then CO_2 flow rate. With both flow rate and surface division being proportional, the same results are obtained when expressed on the cumulated total flow rate and culture surface. Consequently, the only interest of using a multistage system in parallel is in terms of operation. When compared to a single system, similar performances will be obtained, but operating several systems in parallel will be more convenient for maintenance and be more robust with regard to the risk of culture failure, as some systems could be stopped while keeping other systems active to treat CO_2 from flue gas (which could be particularly relevant if the CO_2 emission is rarely stopped as in most industrial plants).

Combination of culture system configurations (simulation D): Obviously, configurations can be mixed. To illustrate that, an association of large culture system followed by a multistage system in series was simulated. The large culture system was retained to correspond to the surface of the first four stages of the multistage (1200 m^2), with those four stages being proven to lead to the same results as a single system of the same size. Results are shown in Figure 9 (black triangle). In addition to the decrease of the number of units that could decrease the total engineering cost, it must be noted that performances were slightly affected when compared to the previous multistage system composed of culture systems of the same surface. Intermediate results are obtained, with a CO_2 removal yield higher than with a single system and a biomass production higher than the one obtained with the previous multistage system. Despite the low performance, it illustrates the potential of our model to investigate various configurations depending on engineering or other constraints.

Relevance of the biological fixation in CO_2 removal: Finally, two additional simulations were conducted without considering microalgal growth to quantify the role of carbon biofixation on CO_2 abatement. The CO_2 removal was then the only result of physical dissolution in the liquid phase (gas−liquid mass transfer) without CO_2 biofixation. The influence of microalgae uptake for photosynthesis is here clearly emphasized. The best efficiency was obtained for the multistage system in series (confirming the advantage of such a concept when compared to a single system), but it remains significantly lower than the one achieved with microalgal culture systems. To achieve 90% CO_2 removal yield, at least 4000 m^2 was necessary (2000 m^2 with microalgae culture).

Interest of Modeling for the In-Depth Understanding of CO_2 Use in Complex Arrangement of Culture Systems. In this final section, a detailed analysis is given to illustrate the interest of modeling to investigate the difference in performances between configurations. Results for single and multistage system in series are given as a function of total surface culture in Table 3 (same results for the single and multistage system in parallel). For a surface below 2400 m^2, a nonlimiting DIC concentration is obtained, with then the maximal CO_2 biofixation rate. The impact of growth limitation by the carbon source appears at 3200 m^2, where 93.7% of the maximum carbon biofixation rate is obtained (with 6.3% loss of productivity compared to the maximal one as permitted by the light supply). Increasing the surface will then reduce the efficiency of the culture system in terms of biomass productivity but will allow decreasing CO_2 content in the outflow. This could be of interest in the aim of purifying the gas in CO_2. For 4000 m^2, a CO_2 content of 0.05% would be reached at the outflow, with a loss of biomass productivity of 24% when compared to the maximum biomass production that could be achieved.

https://doi.org/10.1021/acssuschemeng.2c03927
ACS Sustainable Chem. Eng. 2022, 10, 12826−12842

In contrast to the single-system configuration whose behavior is rather straightforward as it follows similar rules of any culture system fed by a given CO_2 enriched gas phase (i.e., similar to the torus-shaped and airlift PBR, for example), the configuration in series requires a deeper analysis. The behavior of each culture system will be the result of the previous stage that will feed it. Results are given in Figure 10 in terms of performances (CO_2 biofixation rate and CO_2 removal yield; Figure 10a) and CO_2-related operating conditions (DIC concentration in the medium and CO_2 content in the gas phase; Figure 10b). All data are expressed for each stage in the series (i.e., 400 m^2 of surface per stage).

In the first three stages, CO_2 injected allows optimal growth of the biomass (Figure 10a) with a DIC concentration always greater than 10 mM (Figure 10b). We can nevertheless notice that the CO_2 abatement in the gas phase is relatively low (28% for stage #1) and increases as the concentration of DIC in the medium decreases (i.e., increase in gas−liquid mass transfer). The maximum CO_2 removal yield is reached from stage #5, also corresponding to a carbon-limited culture (65% of the maximal biomass biofixation rate). By analogy to the previous studies on lab-scale PBR, a culture system composed of four stages corresponds to the optimal operating conditions, leading to CO_2 removal yield close to maximal ones (as permitted by this configuration) with still optimal growth conditions (>90% of biofixation rate, Figure 10a). For the next stages (#5 to #10), the CO_2 content in the gas phase is insufficient: the DIC concentration is less than 1 mM, and the carbon biofixation rate drops from almost 100% for stage #4 to 65 and 3% for stage #7 and #10, respectively. CO_2 removal yield in the gas phase is therefore maximal (47%) because the low concentration of DIC makes it possible to increase the driving force between the liquid and gas phases. But biomass growth is strongly limited, with very low biomass production. As a result, stages after stage #5 are rather ineffective in terms of biomass production.

The CO_2 removal from the gas phase is related not only to the biomass assimilation but also to the dissolution in the liquid phase. The model allows determining each contribution, and they were added in Figure 10a by adding the part of the CO_2 only assimilated by the biomass (black dotted line). For the first four stages (stage #1−#4), the CO_2 assimilated by the biomass is lower than the CO_2 removal yield, which indicates an accumulation of inorganic carbon in the form of DIC (as also shown in Figure 10b). For example, the decrease in CO_2 in the gas phase of stage #1 is equal to 28%. A third of the injected gaseous CO_2 is then transferred to the liquid phase, but only 13% is biofixed by the biomass, the rest being present in the form of DIC. Then, the CO_2 in the gas phase gradually decreases from stage to stage until it becomes insufficient to obtain nonlimited growth by the carbon source. In those conditions (from stage #5), almost all of the transferred carbon is used by the biomass, and the carbon removal is almost fully explained by biological fixation. Such direct relation between physical (i.e., gas−liquid mass transfer) and biological (i.e., photosynthesis) carbon fluxes was already shown (see Figure 2 for example). Consequently, because the CO_2 transferred from the gas to the liquid phase decreases for the last stages, a very marked decrease in the carbon biofixation yield is observed. The growth kinetic is then directly related to the ability of the process to transfer CO_2, as also already observed in Le Gouic et al.[5] but here in the more complex case of a multistage system.

Discussion on Single vs Multistage Series Configuration on CO_2 Use. The analysis per stage also allows explaining the behavior of the multistage configurations in series compared to others. In the first stages, although a maximal biomass production per stage is obtained, large quantities of carbon are transferred in the liquid phase, which then go out of the system through the liquid outflow. It results in a larger CO_2 removal from the gas phase, with then a better efficiency when compared to a single system of the same area. But after a few stages (five in our simulated case), the CO_2 enrichment in the gas phase becomes too low and growth limiting conditions are obtained: as a result, biomass production capacity drops quickly as well as the CO_2 fixed into biomass. The combination of those two effects (loss of carbon through the liquid phase in first stages and strong growth limitation by the carbon source in the last ones) explains the lower capacity in biomass production for large surfaces when compared to single or multiple systems in parallel of similar surface. Using single or multiple systems indeed avoids this progressive loss of carbon in the liquid outflow. If a sufficient culture area is available, they enable production of roughly the biomass amount permitted stoichiometrically by the CO_2 available in the flue gas. In the case of a limited surface available (below 1500 m^2 in our case), the configuration in series is better as it allows similar biomass production with larger CO_2 removal yield.

CONCLUSIONS

A model allowing predicting CO_2 mass fluxes in microalgae culture systems including kinetic limitation effects on growth has been developed and validated. Its use in simulation enabled us to highlight several aspects, such as the compromise between carbon biofixation and CO_2 removal, or the effect of several typical operating conditions, such as carbon enrichment in the gas and liquid phases (precarbonation), the choice of mixing or cultivation technology (airlift, mechanically stirred PBR, open or covered raceway), or culture system arrangement (single, series, parallel).

In particular, it was possible to highlight the very strong coupling between gas flow rate, gas−liquid mass transfer performance (k_La value), biomass growth rate, and CO_2 content in the gas (input and output), which ultimately leads to a difficulty of optimization.

Considering carbon biofixation rates of the same magnitude (i.e., different culture systems with roughly the same specific illuminated area a_{light} and the same irradiation conditions), we demonstrated that the airlift technology that exhibits high k_La values could be used to ensure a high DIC content and then efficiently prevent inorganic carbon limitations. In contrast, this technology requires generally high gas flow rates for efficient mixing, and then, the output CO_2 content in the gas phase will be often high and slightly different from the input value. For an airlift operated with high content or even pure CO_2 in the gas phase as commonly used in the field, only 1% of CO_2 use efficiency could be obtained. In this context, an optimization of the CO_2 gas phase enrichment according to the parameters of the airlift (k_La, flow rate, biomass growth) would make it possible to significantly reduce CO_2 consumption (i.e., a CO_2 removal yield up to 30−40% was obtained) and therefore operating costs.

The model has also been applied to the case of raceway technology. The covered design turned out to be interesting for better carbon use (with or without combination to a precarbonation) while allowing control of conditions (i.e., bacterial contamination) like any closed technology. The k_La value was also found to be a critical parameter. With gas−liquid

https://doi.org/10.1021/acssuschemeng.2c03927
ACS Sustainable Chem. Eng. 2022, 10, 12826−12842

mass transfer intensification, very high CO_2 removal yields (>80%) were obtained. This is possible here because mechanically stirred technologies enable one to operate with low gas flow rates, leading to more efficient CO_2 abatement in the gas phase. This technology therefore appears ultimately relevant in the context of optimal CO_2 recovery, especially when compared to the airlift technology. Nevertheless, it must be kept in mind that raceways exhibit generally lower biomass and CO_2 volumetric rates than more refined technologies of photobioreactors, leading to higher volumes when sizing the culture system for a given CO_2 flow treatment. In any case, it is always difficult to convert more than a few percent (absolute value) of the CO_2 injected considering biofixation rates limited by light transfer.

By the way, the potential of the model as a tool to scale culture systems or simulate different configurations of single and multistage culture systems was illustrated for a typical flue gas (16% in CO_2). When compared to same systems without algae, the major role of photosynthetic growth as a carbon sink has been shown by allowing in our simulated case to save 50% of the surface for the same CO_2 removal yield. With sufficient surface area, complete purification can be achieved while maximizing the biomass produced. Comparison between different configurations reveals the potential of the single-stage system when large areas were available, with a larger biomass production and almost 100% CO_2 removal efficiency (obtained for a system of 3600 m^2 in our case). Multisystems in parallel lead to the same results but with a benefit in terms of operation as some systems could be stopped while keeping other systems active to treat CO_2 from flue gas. The multistage system in series proved more attractive only when limited areas are available (below 1500 m^2 in our case) because of better CO_2 removal yields for the first stages when compared to a single system (or multistage system in parallel) of the same surface. However, this also results in a quicker decrease in the CO_2 enrichment in the gas phase leading to growth limiting conditions in the following stages and therefore to a quick drop in biomass production and CO_2 biofixation capacity.

Main perspectives of future work will concern the extension of the model to the dynamic case, in particular to simulate solar conditions in the general context of CO_2 mitigation by microalgae (i.e., large-scale solar culture). The improvement of the biological model with respect to the effects of carbon limitation on growth and metabolism will also be considered. Coupling wastewater treatment with CO_2 bioremediation could also be of interest. Our model should be further developed to take into account organic carbon influence on the biological response and carbon fluxes in the process, such as additional CO_2 production due to mixotrophic growth.

AUTHOR INFORMATION

Corresponding Author

Jeremy Pruvost − *Nantes Université, ONIRIS, CNRS, GEPEA, UMR 6144, Saint Nazaire F-44600, France*; orcid.org/0000-0001-9502-1207; Phone: (33) (0)2 40 17 26 69; Email: jeremy.pruvost@univ-nantes.fr; Fax: (33) (0)2 40 17 26 18

Authors

Benjamin Le Gouic − *Nantes Université, ONIRIS, CNRS, GEPEA, UMR 6144, Saint Nazaire F-44600, France*

Jean-François Cornet − *Université Clermont Auvergne, Clermont Auvergne INP, CNRS, Institut Pascal, Clermont-Ferrand F-63000, France*

Complete contact information is available at: https://pubs.acs.org/10.1021/acssuschemeng.2c03927

Author Contributions

Jeremy Pruvost: Conceptualization; Data curation; Formal analysis; Methodology; Supervision; Validation; Writing - review & editing. Benjamin Le Gouic: Data curation; Investigation; Validation; Writing - review & editing. Jean-François Cornet: Conceptualization; Methodology; Writing - review & editing.

Notes

The authors declare no competing financial interest.

ACKNOWLEDGMENTS

This work has been sponsored by the ADEME Project CIMENTALGUE and a public grant of the French National Research Agency as a part of the "Investissements d'Avenir" through the IMobS^3 Laboratory of Excellence (ANR-10-LABX-16-01) and the IDEX-ISITE initiative CAP 20-25 (ANR-16-IDEX-0001).

NOMENCLATURE

a, exchange interfacial area per unit of culture volume [m^{-1}]
C, concentration [$mol \cdot m^{-3}$]
C^*, solubility of CO_2 (given by Henry's law) [$mol \cdot m^{-3}$]
G, gas molar flow rate [$mol \cdot s^{-1}$]
H, Henry's constant [Pa]
K, constant for CO_2/DIC conversion [dimensionless]
K_{DIC}, saturation constant related to growth limitation by DIC concentration [$mol \cdot m^{-3}$]
k_La, overall volumetric mass transfer coefficient [s^{-1} or h^{-1}]
M_i, molar mass for species i [$kg_i \cdot mol_i^{1}$]
N, volumetric molar flux density between liquid and gaseous phases [$mol \cdot m^{-3} \cdot s^{-1}$]
P, total pressure [Pa]
P_X, biomass volumetric productivity [$kg \cdot m^{-3} \cdot s^{-1}$]
$\langle r \rangle$, volumetrical rate, expressed in mole [$mol \cdot m^{-3} \cdot s^{-1}$]
$\langle r' \rangle$, volumetrical rate, expressed in mass [$kg \cdot m^{-3} \cdot s^{-1}$]
t, time [s]
V_L, liquid volume [m^3]
y, molar fraction in gas phase
Y_{CO_2}, yield of biological consumption of CO_2

Greek Letters

η CO_2 removal yield (gas phase)
τ_p residence time (=1/D, with D the dilution rate)
Γ growth kinetic C-efficiency (%)

Subscripts and Superscripts

y^o_{CO2} when used in superscript, related to a reference to output mole fraction
y^i_{CO2} when used in superscript, related to a reference to input mole fraction
i related to the input
o related to the output
G related to gas phase
L related to liquid phase
LL related to light limitation
T related to total concentration (DIC concentration)
X related to biomass

https://doi.org/10.1021/acssuschemeng.2c03927
ACS Sustainable Chem. Eng. 2022, 10, 12826−12842

Abbreviations

PBR photobioreactor
DIC dissolved inorganic carbon

REFERENCES

(1) Benemann, J. R. CO_2 mitigation with microalgae systems. *Energy Convers. Manage.* **1997**, *38*, 475−479.
(2) Eriksen, N. T.; Riisgård, F. K.; Gunther, W. S.; Lønsmann Iversen, J. J. On-line estimation of O_2 production, CO_2 uptake, and growth kinetics of microalgal cultures in a gas-tight photobioreactor. *J. Appl. Phycol.* **2007**, *19*, 161−174.
(3) Keffer, J. E.; Kleinheinz, G. T. Use of chlorella vulgaris for CO_2 mitigation in a photobioreactor. *J. Ind. Microbiol. Biotechnol.* **2002**, *29*, 275.
(4) Takano, H.; Takeyama, H.; Nakamura, N.; Sode, K.; Burgess, J. G.; Manabe, E.; Hirano, M.; Matsunaga, T. CO_2 removal by high density culture of a marine cyanobacterium using an improved photobioreactor employing light-diffusing optical fibers. *Appl. Biochem. Biotechnol.* **1992**, *34-35*, 449−458.
(5) Le Gouic, B.; Marec, H.; Pruvost, J.; Cornet, J. F. Investigation of growth limitation by CO2 mass transfer and inorganic carbon source for the microalga Chlorella vulgaris in a dedicated photobioreactor. *Chem. Eng. Sci.* **2021**, *233*, 116388.
(6) Ifrim, G. A.; Titica, M.; Cogne, G.; Boillereaux, L.; Legrand, J.; Caraman, S. Dynamic pH model for autotrophic growth of microalgae in photobioreactor: A tool for monitoring and control purposes. *AIChE J.* **2014**, *60*, 585−599.
(7) Judd, S. J.; Al Momani, F. A. O.; Znad, H.; Al Ketife, A. M. D. The cost benefit of algal technology for combined CO2 mitigation and nutrient abatement. *Renewable Sustainable Energy Rev.* **2017**, *71*, 379−387.
(8) Watanabe, Y.; Saiki, H. Development of a photobioreactor incorporating Chlorella sp. for removal of CO_2 in stack gas. *Energy Convers. Manage.* **1997**, *38*, 499−503.
(9) Cheng, L.; Zhang, L.; Chen, H.; Gao, C. Carbon dioxide removal from air by microalgae cultured in a membrane-photobioreactor. *Sep. Purif. Technol.* **2006**, *50*, 324−329.
(10) Cornet, J. F.; Dussap, C. G.; Gros, J. B.; Binois, C.; Lasseur, C. A simplified monodimensional approach for modeling coupling between radiant light transfer and growth kinetics in photobioreactors. *Chem. Eng. Sci.* **1995**, *50*, 1489−1500.
(11) Dauchet, J.; Cornet, J.-F.; Gros, F.; Roudet, M.; Dussap, C.-G. Photobioreactor modeling and Radiative Transfer Analysis for engineering puposes. *Adv. Chem. Eng. J.* **2016**, *48*, 1−106.
(12) Pottier, L.; Pruvost, J.; Deremetz, J.; Cornet, J. F.; Legrand, J.; Dussap, C. G. A fully predictive model for one-dimensional light attenuation by Chlamydomonas reinhardtii in a torus photobioreactor. *Biotechnol. Bioeng.* **2005**, *91*, 569−582.
(13) Pruvost, J.; Cornet, J. F. Knowledge models for engineering and optimization of photobioreactors. In *Microalgal Biotechnology*, Walter, C. P. A. Ed.; De Gruyter GmbH & Co. KG, 2012; pp. 181−224.
(14) Pruvost, J.; Le Borgne, F.; Artu, A.; Cornet, J.-F.; Legrand, J. Industrial Photobioreactors and Scale-Up Concepts. In *Advances in Chemical Engineering - Photobioreaction Engineering*, Vol. *48*; Elsevier, 2016; pp. 257−310.
(15) Takache, H.; Pruvost, J.; Cornet, J. F. Kinetic modeling of the photosynthetic growth of Chlamydomonas reinhardtii in a photobioreactor. *Biotechnol. Prog.* **2012**, *28*, 681−692.
(16) Soulies, A.; Legrand, J.; Marec, H.; Pruvost, J.; Castelain, C.; Burghelea, T.; Cornet, J. F. Investigation and modeling of the effects of light spectrum and incident angle on the growth of *Chlorella vulgaris* in photobioreactors. *Biotechnol. Prog.* **2016**, *32*, 247−261.
(17) Pruvost, J.; Van Vooren, G.; Cogne, G.; Legrand, J. Investigation of biomass and lipids production with *Neochloris oleoabundans* in photobioreactor. *Bioresour. Technol.* **2009**, *100*, 5988−5995.
(18) Cornet, J. F.; Dussap, C. G.; Cluzel, P.; Dubertret, G. A structured model for simulation of cultures of the cyanobacterium *Spirulina platensis* in photobioreactors. II. Identification of kinetic parameters under light and mineral limitations. *Biotechnol. Bioeng.* **1992**, *40*, 826−834.
(19) Moroney, J. V.; Jungnick, N.; DiMario, R. J.; Longstreth, D. J. Photorespiration and carbon concentrating mechanisms: two adaptations to high O_2, low CO_2 conditions. *Photosynth. Res.* **2013**, *117*, 121−131.
(20) Kazbar, A.; Cogne, G.; Urbain, B.; Marec, H.; Le-Gouic, B.; Tallec, J.; Takache, H.; Ismail, A.; Pruvost, J. Effect of dissolved oxygen concentration on microalgal culture in photobioreactors. *Algal Res.* **2019**, *39*, 101432.
(21) Martzolff, A.; Cahoreau, E.; Cogne, G.; Peyriga, L.; Portais, J. C.; Dechandol, E.; Le Grand, F.; Massou, S.; Gonçalves, O.; Pruvost, J.; Legrand, J. Photobioreactor design for isotopic non-stationary 13C-metabolic flux analysis (INST 13C-MFA) under photoautotrophic conditions. *Biotechnol. Bioeng.* **2012**, *109*, 3030−3040.
(22) Loubiere, K.; Pruvost, J.; Aloui, F.; Legrand, J. Investigations in an external-loop airlift photobioreactor with annular light chambers and swirling flow. *Chem. Eng. Res. Des.* **2011**, *89*, 164−171.
(23) Loubière, K.; Olivo, E.; Bougaran, G.; Pruvost, J.; Robert, R.; Legrand, J. A new photobioreactor for continuous microalgal production in hatcheries based on external-loop airlift and swirling flow. *Biotechnol. Bioeng.* **2009**, *102*, 132−147.
(24) Janssen, M.; De Bresser, L.; Baijens, B.; Tramper, J.; Mur, L. R.; Snel, J.; Wijffels, R. H. Scale-up aspects of photobioreactors: effects of mixing-induced light/dark cycles. *J. Appl. Phycol.* **2000**, *12*, 225−237.
(25) Ranjbar, R.; Inoue, R.; Katsuda, T.; Yamaji, H.; Katoh, S. High efficiency production of astaxanthin in an airlift photobioreactor. *J. Biosci. Bioeng.* **2008**, *106*, 204−207.
(26) Fernandes, B. D.; Dragone, G. M.; Teixeira, J. A.; Vicente, A. A. Light regime characterization in an airlift photobioreactor for production of microalgae with high starch content. *Appl. Biochem. Biotechnol.* **2010**, *161*, 218−226.
(27) Weissman, J. C.; Goebel, R. P.; Benemann, J. R. Photobioreactor Design: Mixing, Carbon Utilization, and Oxygen Accumulation. *Biotechnol. Bioeng.* **1988**, *31*, 336−344.
(28) Busnel, A.; Samhat, K.; Gérard, E.; Kazbar, A.; Marec, H.; Dechandol, E.; Le Gouic, B.; Hauser, J. L.; Pruvost, J. Development and validation of a screening system for characterizing and modeling biomass production from cyanobacteria and microalgae: Application to Arthrospira platensis and Haematococcus pluvialis. *Algal Res.* **2021**, *58*, 102386.
(29) Pruvost, J.; Cornet, J. F.; Goetz, V.; Legrand, J. Modeling dynamic functioning of rectangular photobioreactors in solar conditions. *AIChE J.* **2011**, *57*, 1947−1960.
(30) Pruvost, J.; Cornet, J. F.; Le Borgne, F.; Goetz, V.; Legrand, J. Theoretical investigation of microalgae culture in the light changing conditions of solar photobioreactor production and comparison with cyanobacteria. *Algal Res.* **2015**, *10*, 87−99.
(31) Benemann, J. R.; Oswald, W. J. Systems and economics analysis of microalgae ponds for conversion of CO2 to biomass. *Nasa Sti/recon Tech. Rep.* **1996**, 19554.
(32) Cheng, J.; Yang, Z.; Huang, Y.; Huang, L.; Hu, L.; Xu, D.; Zhou, J.; Cen, K. Improving growth rate of microalgae in a 1191 m^2 raceway pond to fix CO_2 from flue gas in a coal-fired power plant. *Bioresour. Technol.* **2015**, *190*, 235−241.
(33) Mortensen, L. M.; Gislerød, H. R. The growth of Chlorella sorokiniana as influenced by CO2, light, and flue gases. *J. Appl. Phycol.* **2016**, *28*, 813−820.
(34) Bird, R. B.; Stewart, W. E.; Lightfoot, E. N. *Transport phenomena* (second edition); John Wiley & Sons, Inc., 2002, DOI: 10.1115/1.1424298.

https://doi.org/10.1021/acssuschemeng.2c03927
ACS Sustainable Chem. Eng. 2022, 10, 12826−12842